Role of large volcanic eruptions on the ENSO and Indian Monsoon Coupling

International Workshop on Stratosphere-Troposphere Interactions

& Prediction of Monsoon Weather Extremes (STIPMEX)

3-7 June 2024, IITM, Pune

R. Krishnan

Indian Institute of Tropical Meteorology, Pune, India

Human influence has warmed the climate at a rate that is unprecedented in at least the last 2000 years

Figure SPM.1

Changes in global surface temperature relative to 1850-1900

a) Change in global surface temperature (decadal average) as reconstructed (1-2000) and **observed** (1850-2020)

b) Change in global surface temperature (annual average) as **observed** and simulated using human & natural and only natural factors (both 1850-2020)

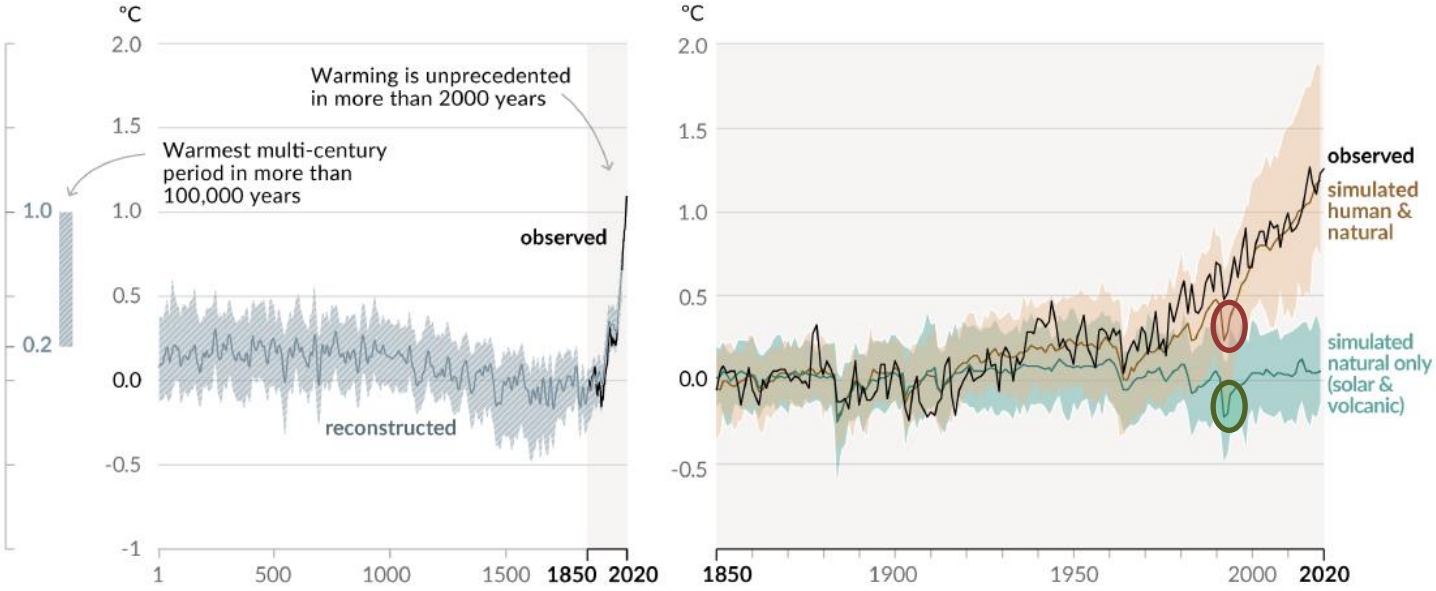

Interactions of two complex dynamical systems

1. Indian Monsoon (IM)
2. El Nino – Southern Oscillation (ENSO)

Whether large volcanic eruptions (LVE) can alter the coupling of IM and ENSO ?

The Indian Summer Monsoon

Complex Dynamical System

Tibetan Plateau

India

Cumulus clouds

Monsoon low-level jet

Equatorial Ocean-Atmosphere Dynamics

Indian Ocean

N

E

W

S

Land-Ocean-Atmosphere Coupled System

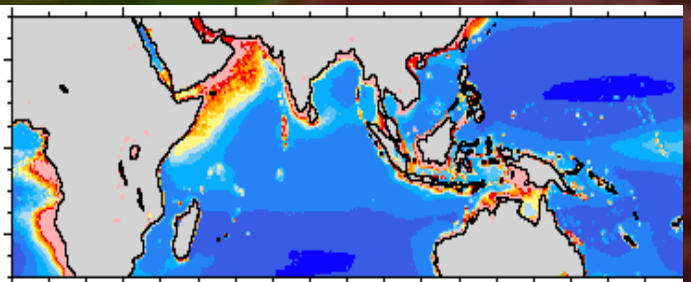

Chlorophyll Conc (Mg m^{-3})
SeaWiFS

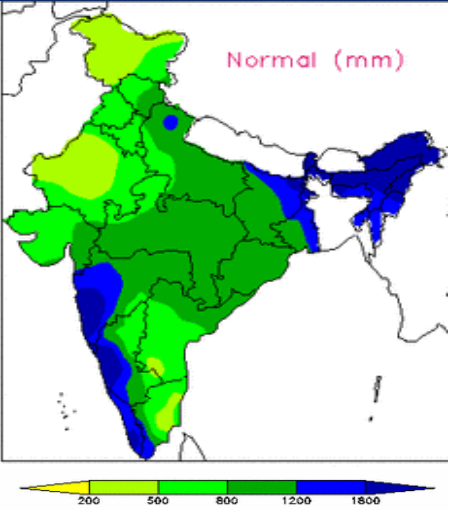

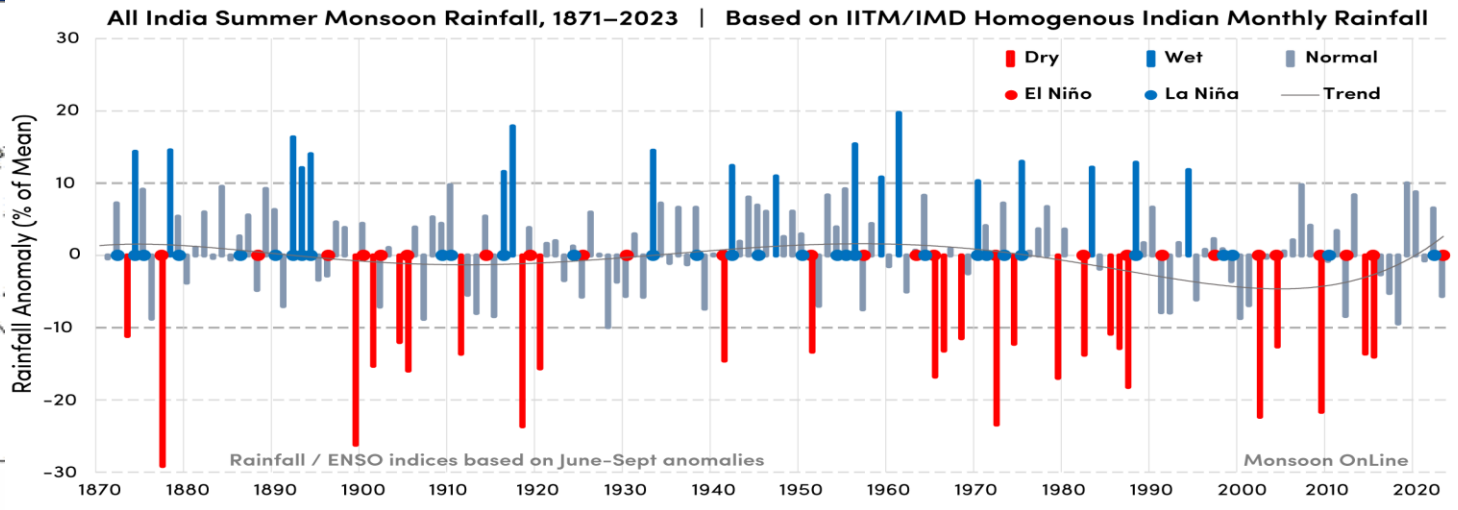

Typical Walker circulation pattern

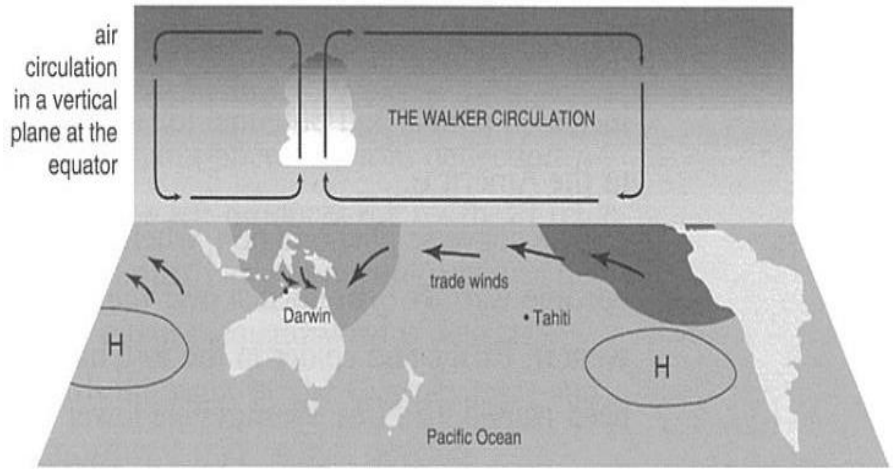

Walker circulation during an El Niño

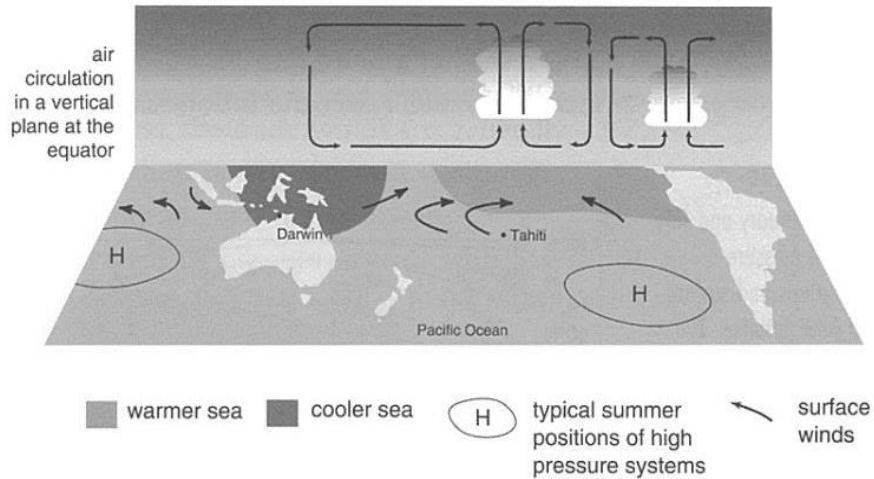

The 1997/98 El Nino – Evolution of ocean temperature and anomalies

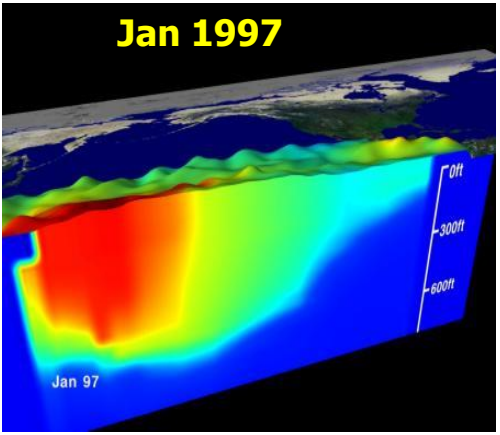

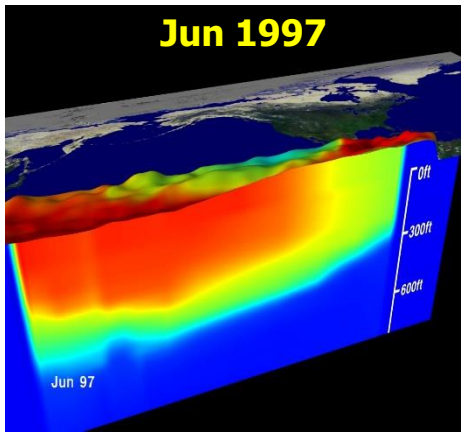

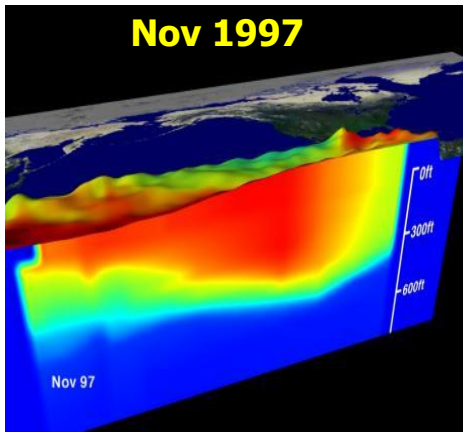

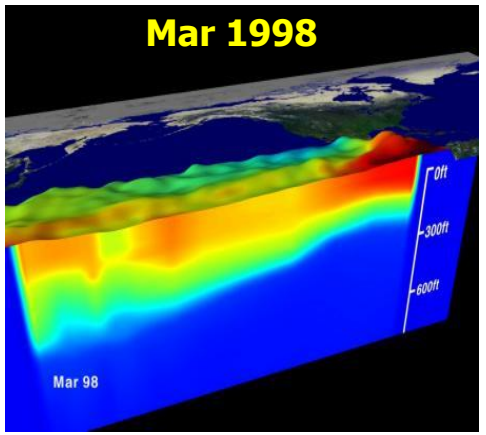

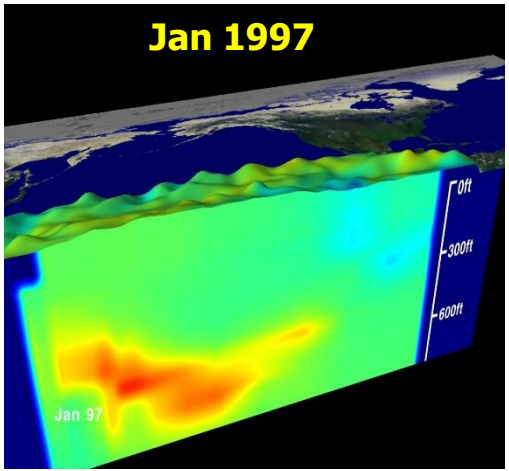

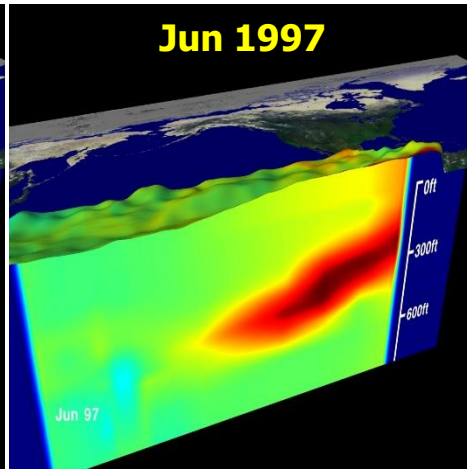

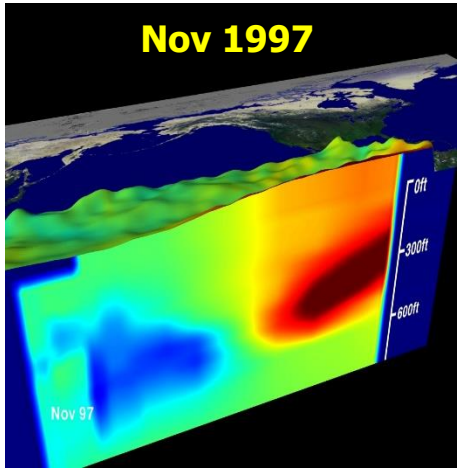

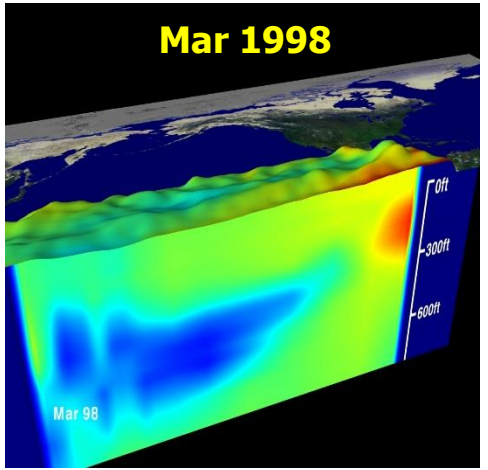

On the Weakening Relationship Between the Indian Monsoon and ENSO

K. Krishna Kumar, Balaji Rajagopalan, Mark A. Cane

Science, 1999

Analysis of the 140-year historical record suggests that the inverse relationship between the El Nino-Southern Oscillation (ENSO) and the Indian summer monsoon (weak monsoon arising from warm ENSO event) has broken down in recent decades. Two possible reasons emerge from the analyses. A southeastward shift in the Walker circulation anomalies associated with ENSO events may lead to a reduced subsidence over the Indian region, thus favoring normal monsoon conditions. Additionally, increased surface temperatures over Eurasia in winter and spring, which are a part of the midlatitude continental warming trend, may favor the enhanced land-ocean thermal gradient conducive to a strong monsoon. These observations raise the possibility that the Eurasian warming in recent decades helps to sustain the monsoon rainfall at a normal level despite strong ENSO events.

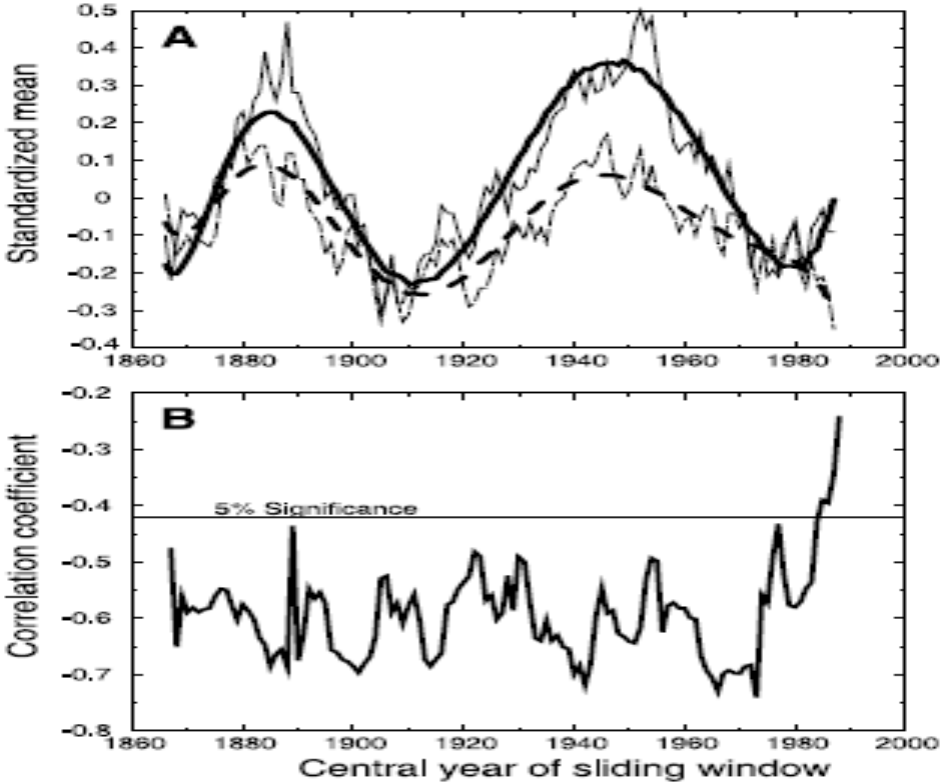

Fig. 1. (**A**) Shown are 21-year sliding standardized means of Indian summer monsoon rainfall (thin line) and June to August (JJA) NINO3 SST anomalies (thin dashed line) during 1856-1997. The corresponding solid lines represent the smoothed values (smoothing is done by fitting a polynomial). The sign of NINO3 SST is reversed to facilitate direct comparison. (**B**) Shown are 21-year sliding correlations between Indian summer monsoon rainfall and NINO3 SST anomalies (JJA) during 1856 - 1997. The horizontal line shows the 5% significance level.

Maraun, D. and Kurths, J., 2005. Epochs of phase coherence between El Nino/Southern Oscillation and Indian monsoon. Geophy Res Lett, 32(15)

- We present a modern method used in nonlinear time series analysis to investigate the relation of two oscillating systems with respect to their phases, independently of their amplitudes.
- We study the difference of the phase dynamics between El Nino/Southern Oscillation (ENSO) and the Indian Monsoon on inter-annual time scales.
- We identify distinct epochs, especially two intervals of phase coherence, 1886–1908 and 1964–1980, corroborating earlier findings from a new point of view.
- A significance test shows that the coherence is very unlikely to be the result of stochastic fluctuations.
- We also detect so far unknown periods of coupling which are invisible to linear methods.
- These findings suggest that the decreasing correlation during the last decades might be a typical epoch of the ENSO/ Monsoon system having occurred repeatedly.
- The high time resolution of the method enables us to present an interpretation of how volcanic radiative forcing could cause the coupling.

Phase Reconstruction

When two systems exhibiting self-sustained oscillations of (at least slightly) different frequencies are brought into contact, one observes, in general, the following phenomena: For a low coupling strength, the systems evolve independently. Increasing the coupling strength, at first the frequencies start to adjust, such that the phases describing the oscillations get locked. This phase coherence phenomenon is called phase synchronization [Rosenblum et al., 1996]. For stronger coupling, generalized synchronization might arise, i.e. the amplitudes might also adjust.

Christiaan Huygens (1629–1695) - Famous Dutch Mathematician, Astronomer & Physicist

$$|\Phi_1(t) - \Phi_2(t)| < \epsilon$$

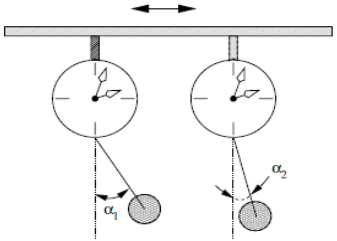

A. Pikovsky, M. Rosenblum, J. Kurths (2001):

Synchronization – A Universal Concept in Nonlinear Sciences

Figure 1.8. Two pendulum clocks coupled through a common support. The beam to which the clocks are fixed is not rigid, but can vibrate slightly, as indicated by the arrows at the top of the figure. This vibration is caused by the motions of both pendula; as a result the two clocks "feel" the presence of each other.

Phase Coherence Analysis (PCA)

Understand the phase relationships between ENSO & IM

Hilbert Transform

$$H(u)(t) = \frac{1}{\pi}\,\mathrm{p.v.}\int_{-\infty}^{+\infty}\frac{u(\tau)}{t-\tau}\,d\tau,$$

P.V. is the Cauchy principal value

Osipov et al. (2003): By geometrical reasoning about the curvature of phase space trajectories, the phase can be derived by considering the time-derivative of the signal

$$\phi = \arctan\frac{\dot{y}}{\dot{x}}$$

- Time series of ENSO and IM are filtered to remove intra-annual oscillations (cutoff = 0.75 cycles per year)
- Second order time differencing followed by Hilbert Transform
- Phase ϕ computed from transformed series $\boxed{\varphi(t) = x(t) + i\,y(t)}$
- $\phi = \tan^{-1}[\, y(t) / x(t) \,]$

Maraun and Kurths (2005)

Maraun, D. and Kurths, J., 2005. Epochs of phase coherence between El Nino/Southern Oscillation and Indian monsoon. Geophys. Res. Lett, 32(15).

Time-series of NINO3 & AIR

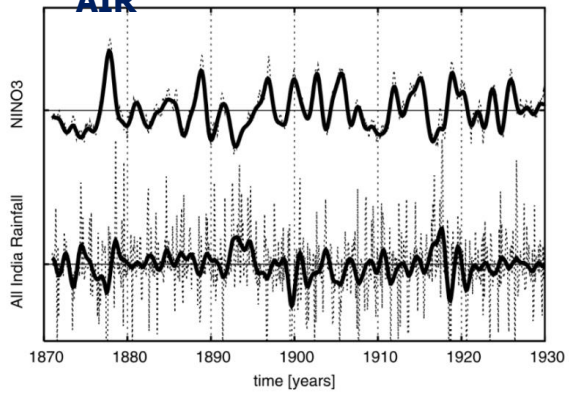

Fig.1 Section of the NINO3 (upper graph) & AIR anomalies (lower graph) time series. The dotted lines depict the raw data, the solid lines show the low-pass filtered data used for the further analysis.

Hilbert Transform NINO3

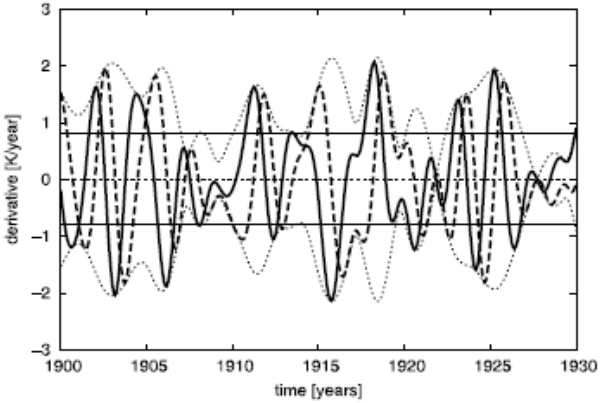

Fig.3. Smoothed derivative of the normalized and lowpass filtered NINO3 time series (solid line, section), the corresponding Hilbert transformation (dashed line). The dotted line represents the amplitude A (for details see text). For A > 0.8 (solid horizontal lines), we consider the phase to be well defined.

Unwrapped ENSO, IM phases from Hilbert Transform

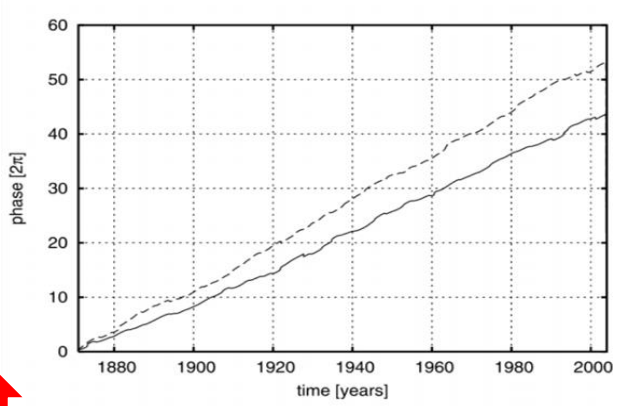

Fig.4 Phase propagation of NINO3 (solid) and Monsoon (dashed). On average, the latter one oscillates faster. However, during some periods the phases propagate similarly, suggesting to investigate for phase coherence.

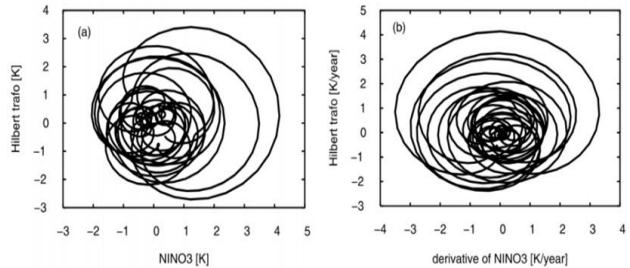

Figure 2. (a) Embedding of low-pass filtered NINO3 time series by Hilbert transformation. Many oscillations are not centered around a common center. (b) The same, but for the time derivative of the NINO3 time series. All pronounced oscillations circle around the origin.

Steps for Phase Reconstruction

1. Low-pass filter the data in the spectral domain. A smooth function (arcus tangens) damping frequencies > 0.7 per year is chosen.

2. Estimate derivatives by second order difference scheme and running mean with window width $2\ell + 1 = 13$ months

3. Embed by Hilbert transformation with phase defined according to equation (3).

4. Unwrap the phases (add 2π after each oscillation)

5. The envelope $A(t) = (\dot{x}(t)^2 + \dot{y}(t)^2)^{1/2}$ is chosen to select regions of well defined phases: For time derivatives x(t) normalized to unit variance, A(t) > 0.8 appeared to be a reasonable choice to exclude spurious oscillations.

ENSO IM phase difference & VRF

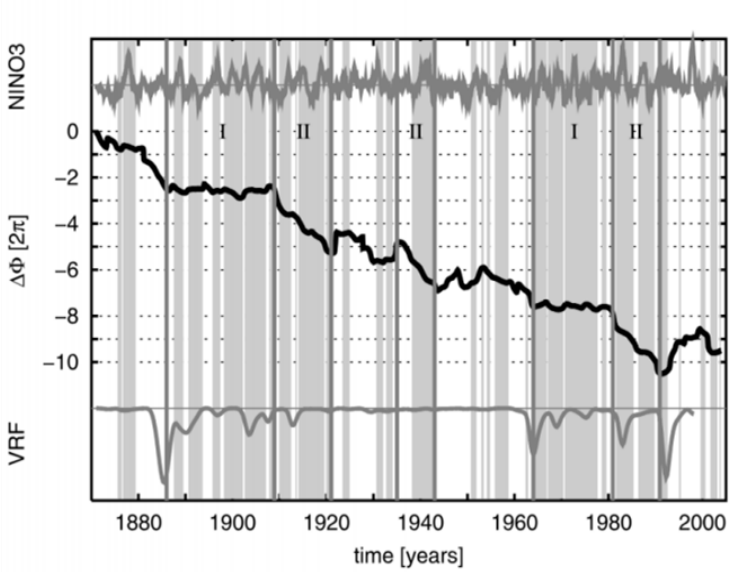

Fig.5 Phase difference of ENSO & Monsoon (black). Grey shading marks intervals of jointly well defined phases. 1886–1908 and 1964–1980 (I): plateaus indicate phase coherence. 1908–1921, 1935–1943 and 1981–1991 (II): Monsoon oscillates with twice the phase velocity of ENSO. During these intervals, both systems exhibit distinct oscillations (NINO3 time series, upper graph). 1921–1935 and 1943–1963: phases are badly defined, both processes exhibit irregular oscillations of low variance (upper graph). Lower graph shows volcanic radiative forcing index (VRF).

Epochs of ENSO-IM Phase Coherence

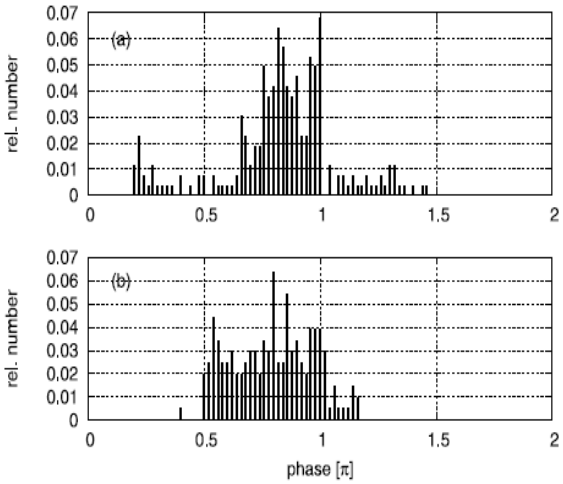

Figure 6. Histogram of phase differences for the two phase coherent intervals (a) 1886–1908, (b) 1964–1980. Both diagrams show peaks between π/2 and π, reflecting that ENSO and Monsoon are anti-correlated.

Maraun, D. and Kurths, J., 2005. Geophys. Res. Lett, 32(15).

Large volcanic eruptions can trigger El Ninos – Khodri et al. 2017

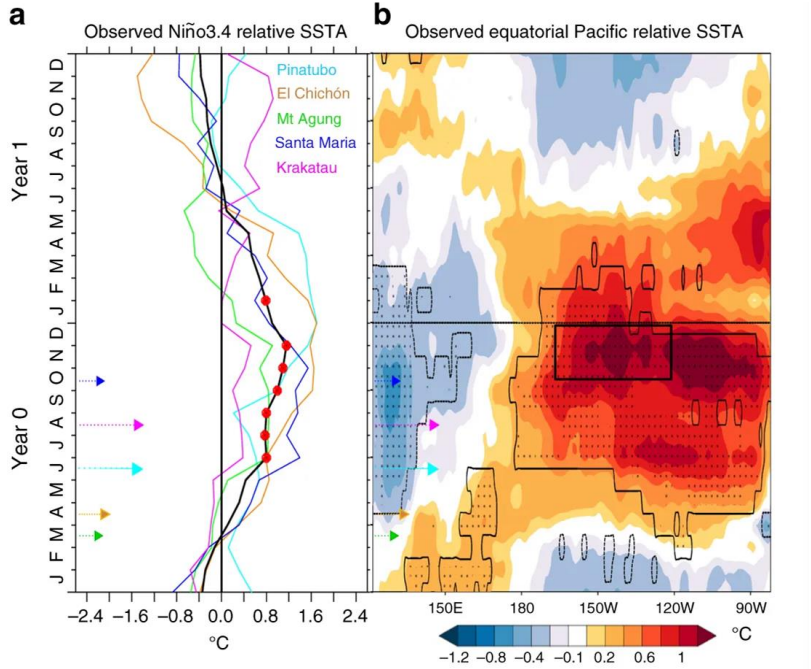

Krakatau - Aug 1883; Santa María - Oct 1902; Mt Agung - Mar 1963, El Chichón - April 1982; Pinatubo - June 1991

Agung eruption 1963-64, Bali, Indonesia. Photograph taken on 16 May 1963

Khodri, M., Izumo, T., Vialard, J., Janicot, S., Cassou, C., Lengaigne, M., Mignot, J., Gastineau, G., Guilyardi, E., Lebas, N. and Robock, A., 2017. Tropical explosive volcanic eruptions can trigger El Niño by cooling tropical Africa. *Nature communications*, *8*(1), pp.1-13.

Schematic of the mechanism for volcanic El Niño development following a Pinatubo-like eruption in June – Khodri et al. 2017

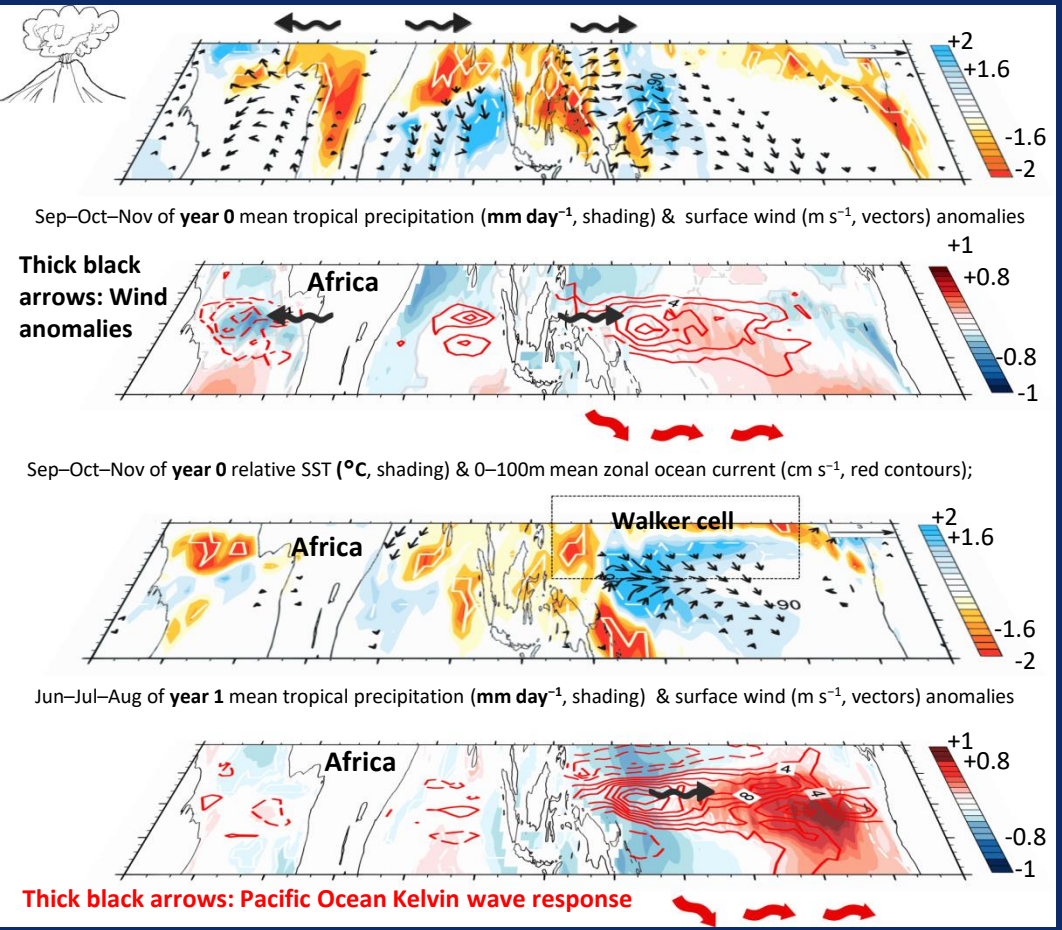

Jun-Jul-Aug of **year 1** relative SST (**°C**, shading) & 0–100m mean zonal ocean current (cm s^{-1}, red contours) after the Pinatubo eruption

June eruption: Reduced tropical precipitation in particular over West Africa favours anomalous atmospheric Rossby and Kelvin waves in August–November

Shoaling of the Atlantic Ocean thermocline. Initiation of anomalous oceanic downwelling Kelvin waves reaching Central Pacific in December of the eruption year

Bjerknes feedback and weakened Pacific Walker circulation by tropical land cooling in August–October

Initiate anomalous downwelling Kelvin waves leading to an El Niño event peaking in fall of the year following the eruption

IPSL-CM5B coupled model ensemble

Khodri et al. 2017

SCIENCE ADVANCES | RESEARCH ARTICLE

GEOLOGY

Fingerprint of volcanic forcing on the ENSO–Indian monsoon coupling

M. Singh[1,2], R. Krishnan[1]*, B. Goswami[3,4], A. D. Choudhury[1], P. Swapna[1], R. Vellore[1], A. G. Prajeesh[1], N. Sandeep[1], C. Venkataraman[2], R. V. Donner[3,5], N. Marwan[3], J. Kurths[3,6]

Coupling of the El Niño–Southern Oscillation (ENSO) and Indian monsoon (IM) is central to seasonal summer monsoon rainfall predictions over the Indian subcontinent, although a nonstationary relationship between the two nonlinear phenomena can limit seasonal predictability. Radiative effects of volcanic aerosols injected into the stratosphere during large volcanic eruptions (LVEs) tend to alter ENSO evolution; however, their impact on ENSO-IM coupling remains unclear. Here, we investigate how LVEs influence the nonlinear behavior of the ENSO and IM dynamical systems using historical data, 25 paleoclimate reconstructions, last-millennium climate simulations, large-ensemble targeted climate sensitivity experiments, and advanced analysis techniques. Our findings show that LVEs promote a significantly enhanced phase-synchronization of the ENSO and IM oscillations, due to an increase in the angular frequency of ENSO. The results also shed innovative insights into the physical mechanism underlying the LVE-induced enhancement of ENSO-IM coupling and strengthen the prospects for improved seasonal monsoon predictions.

PCA of Last Millennium using PMIP3

- NINO3 SST (5°N-5°S, 150°W-90°W) and IM rainfall (74.5°E-86.5°E, 16.5°N-26.5°N) from IPSL model (850 - 1850 AD) used

- Phase space plot oscillating around a common attractor -> ENSO and IM self sustained oscillators -> all theories of phase synchronization applicable on filtered time series

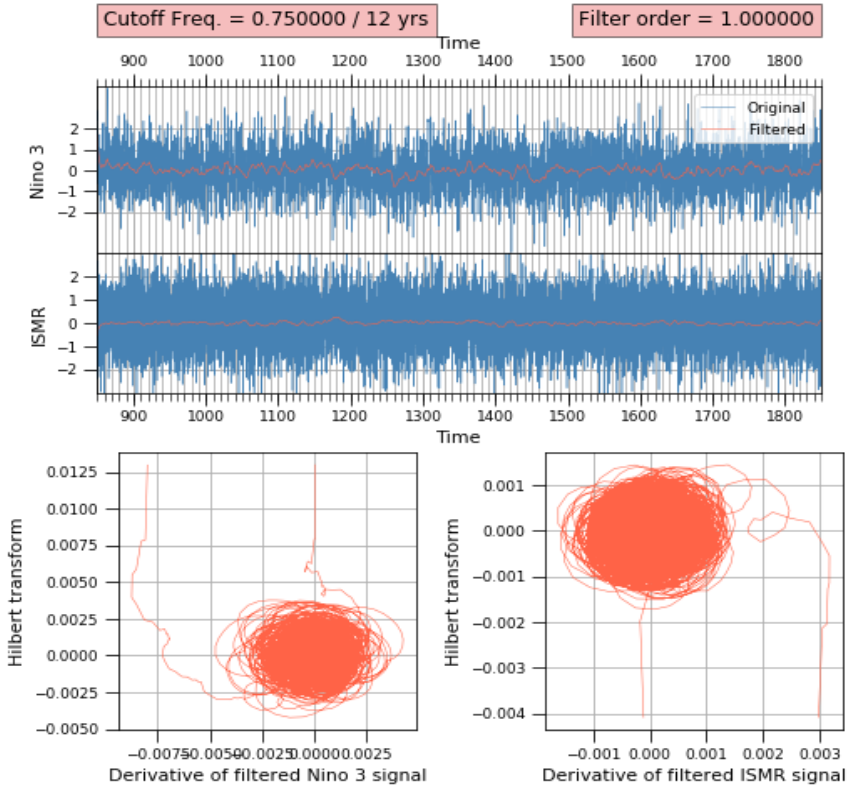

Source: Manmeet Singh et al., 2020

PCA of Last Millennium PMIP3 – IPSL Model

Last Millennium (850-1850)

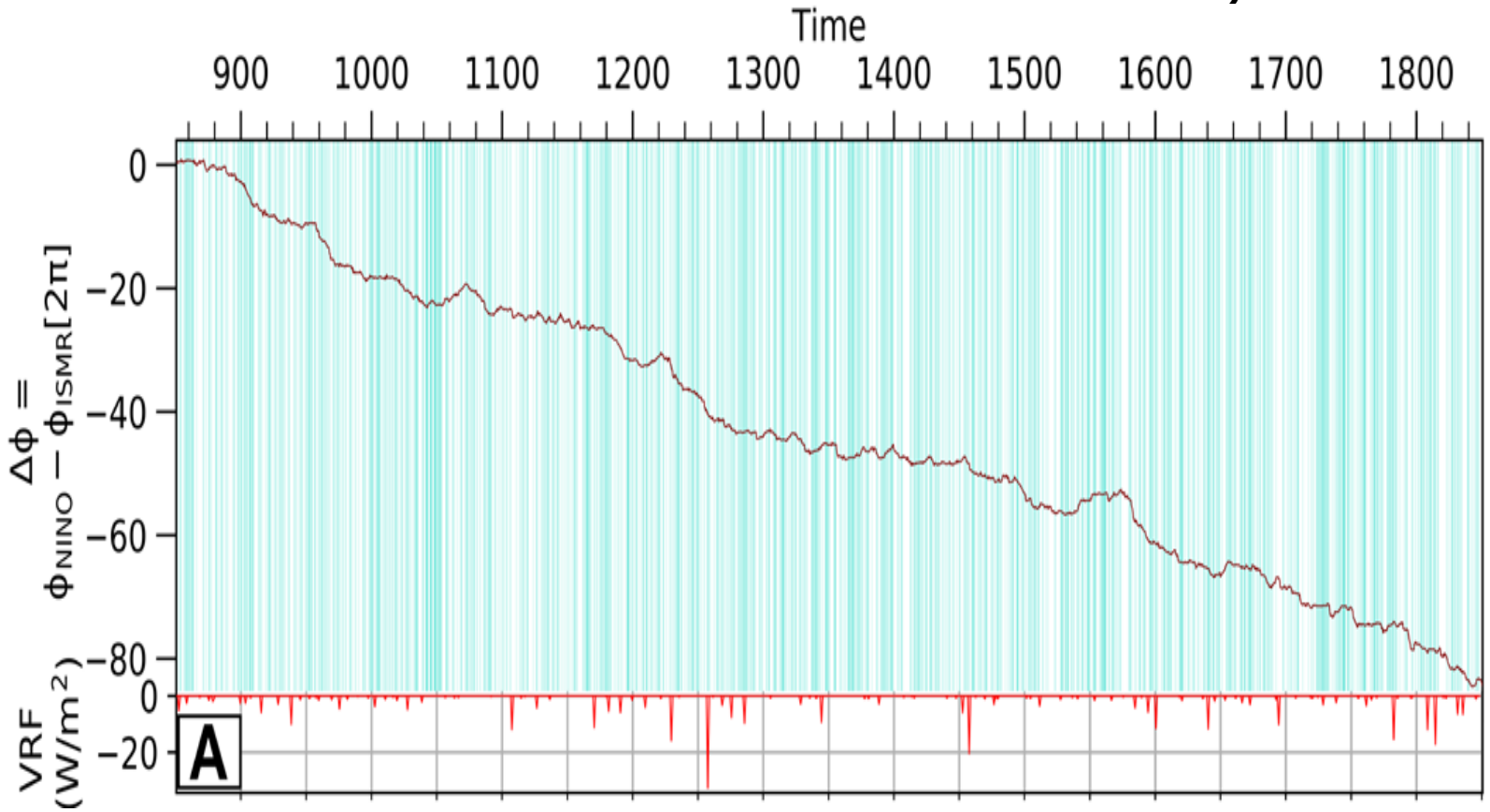

Manmeet Singh et al. 2020

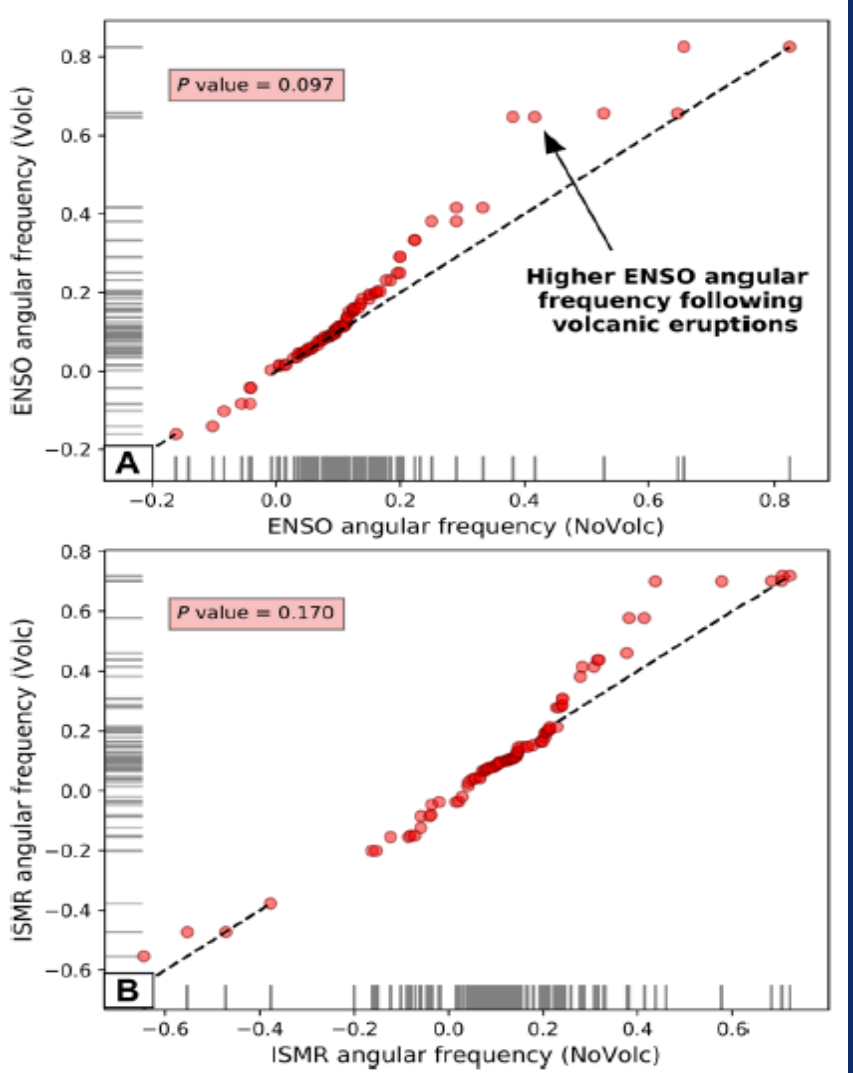

Faster ENSO phase speed following volcanic eruptions

Fig. 2. LVE-induced modulations of the angular frequency of ENSO and IM oscillations during the last millennium (850–1850). Q-Q plot showing angular frequency of (**A**) ENSO and (**B**) IM oscillations based on the volcanic and no volcanic distributions. The volcanic distributions are bootstrapped from year (0) to year (4) relative to volcanic eruption. Angular frequencies are obtained as the first derivative of the instantaneous phase computed using phase coherence analysis of monthly indices of Niño3 and IM precipitation from the IPSL PMIP3 last-millennium simulation. The oscillations of ENSO evolve slowly relative to the IM oscillations, so that increases in the angular frequency of ENSO tend to enhance ENSO-IM phase coherence.

Manmeet Singh et al. 2020

IITM Earth System Model for long term climate studies – the first from India

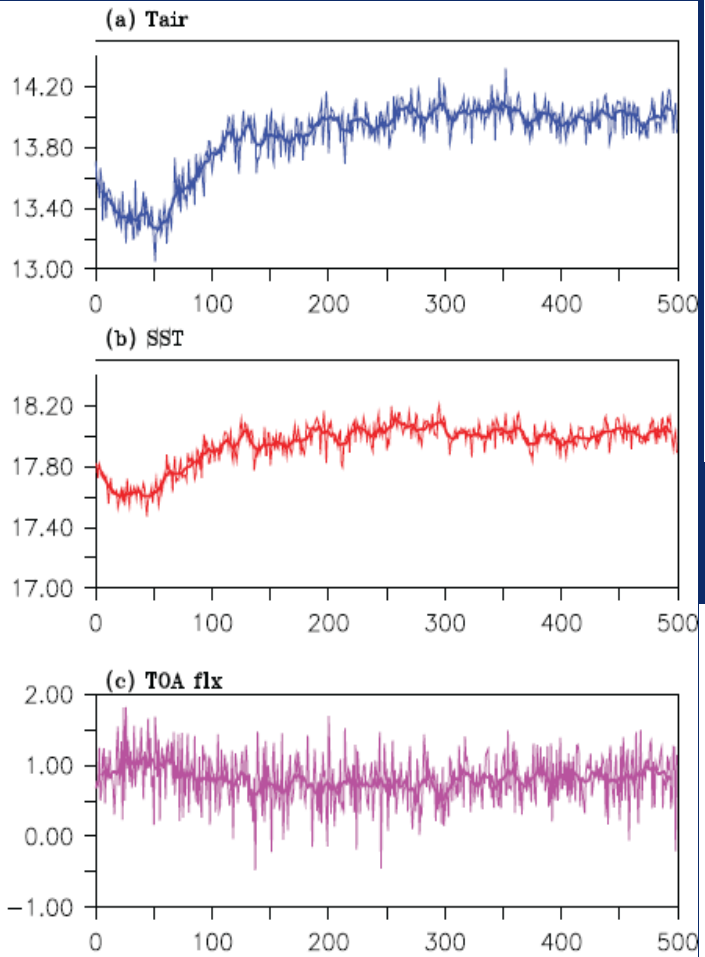

Journal of Advances in Modeling Earth Systems

RESEARCH ARTICLE
10.1029/2017MS001262

Long-Term Climate Simulations Using the IITM Earth System Model (IITM-ESMv2) with Focus on the South Asian Monsoon

P. Swapna[1], R. Krishnan[1], N. Sandeep[1], A. G. Prajeesh[1], D. C. Ayantika[1], S. Manmeet[1], and R. Vellore[1]

Key Points:
- IITM-ESMv2 simulations show fidelity in capturing large-scale circulation

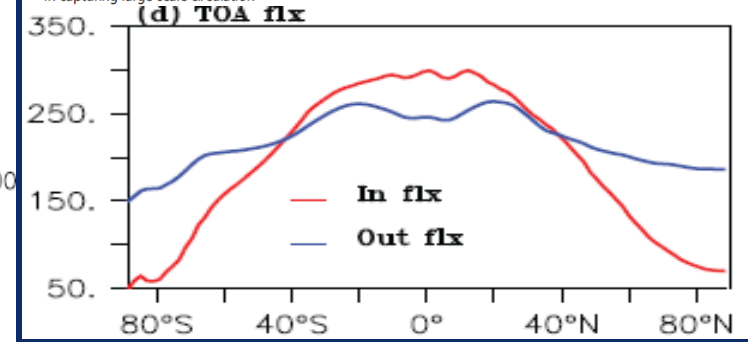

Improved simulation of sea-ice

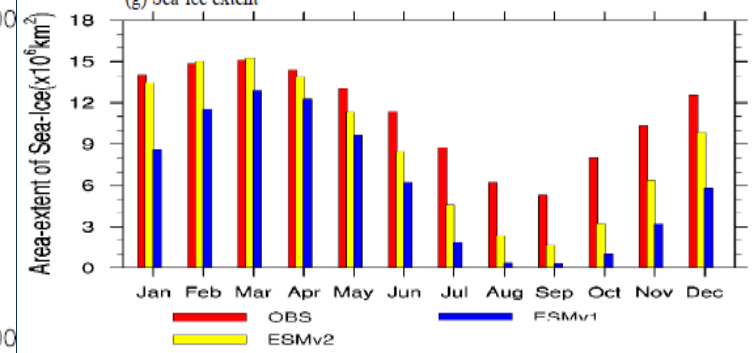

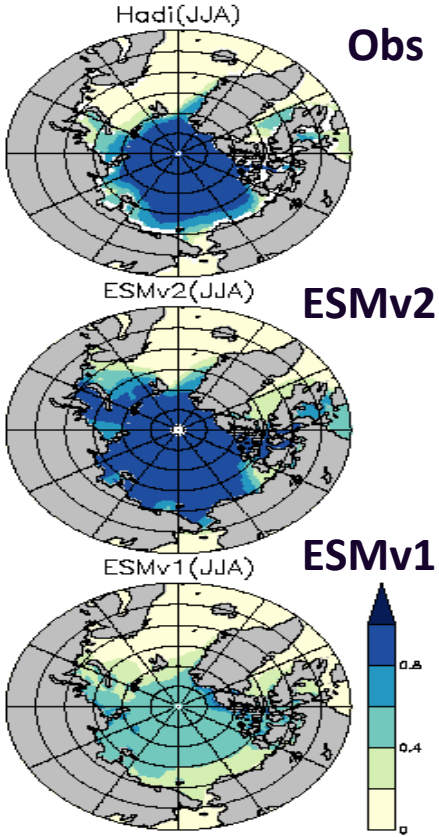

Design of large-ensemble targeted sensitivity experiments using IITM-ESM

Krakatau Eruption - 1883

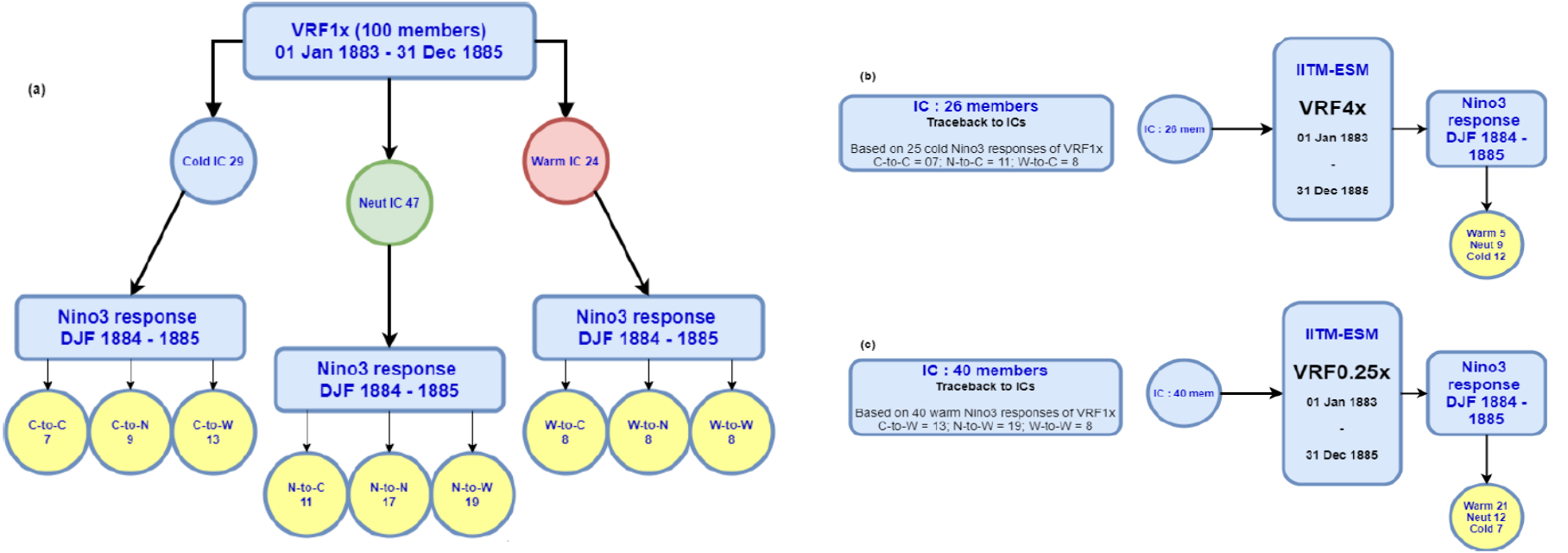

Schematic flowchart of the large-ensemble targeted sensitivity experiments using the IITM-ESM: (a) 100-member ensemble (i.e., 29 cold ICs, 47 Neutral ICs and 24 warm ICs) VRF1x experiments starting from 01 January 1883 through 31 December 1885. The yellow circles are based on the Niño3 response during Dec-Jan-Feb 1884-1885. The acronyms C-to-C, N-to-C, W-to-C … are used to indicate the initial state and the transitioned state during DJF 1884-85. For example the N-to-C green circle corresponds to neutral ICs that transitioned to cold Nino3 anomalies during DJF 1884-85 (b) 26-member (Mem#26) VRF4x ensemble experiment (c) 40-member (Mem#41) VRF0.25x ensemble experiment.

IITM-ESM Large Ensemble Experiments: Volcanic forcing & ENSO-Indian monsoon coupling

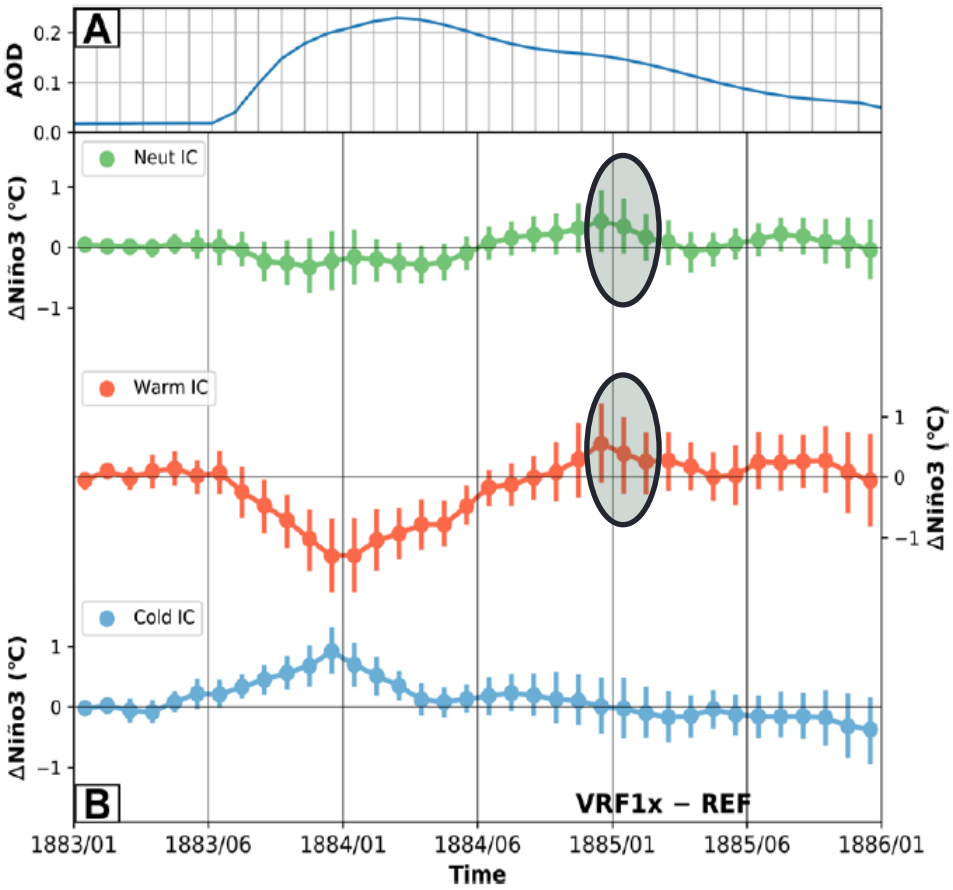

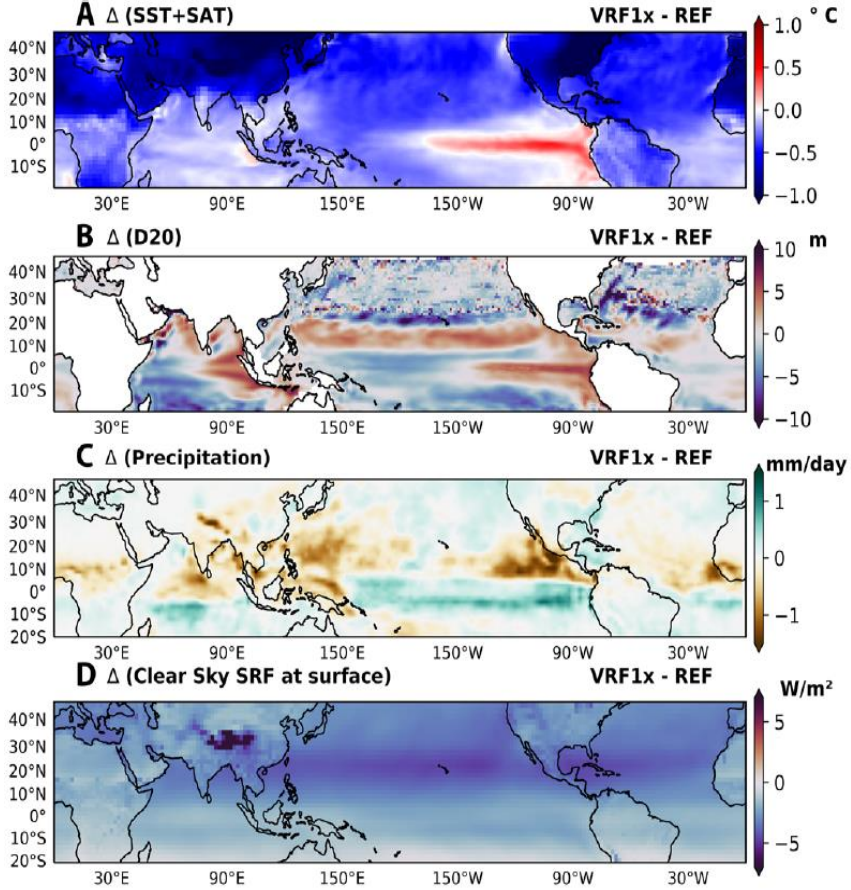

Manmeet Singh et al. 2020

Strength of Volcanic Eruptions

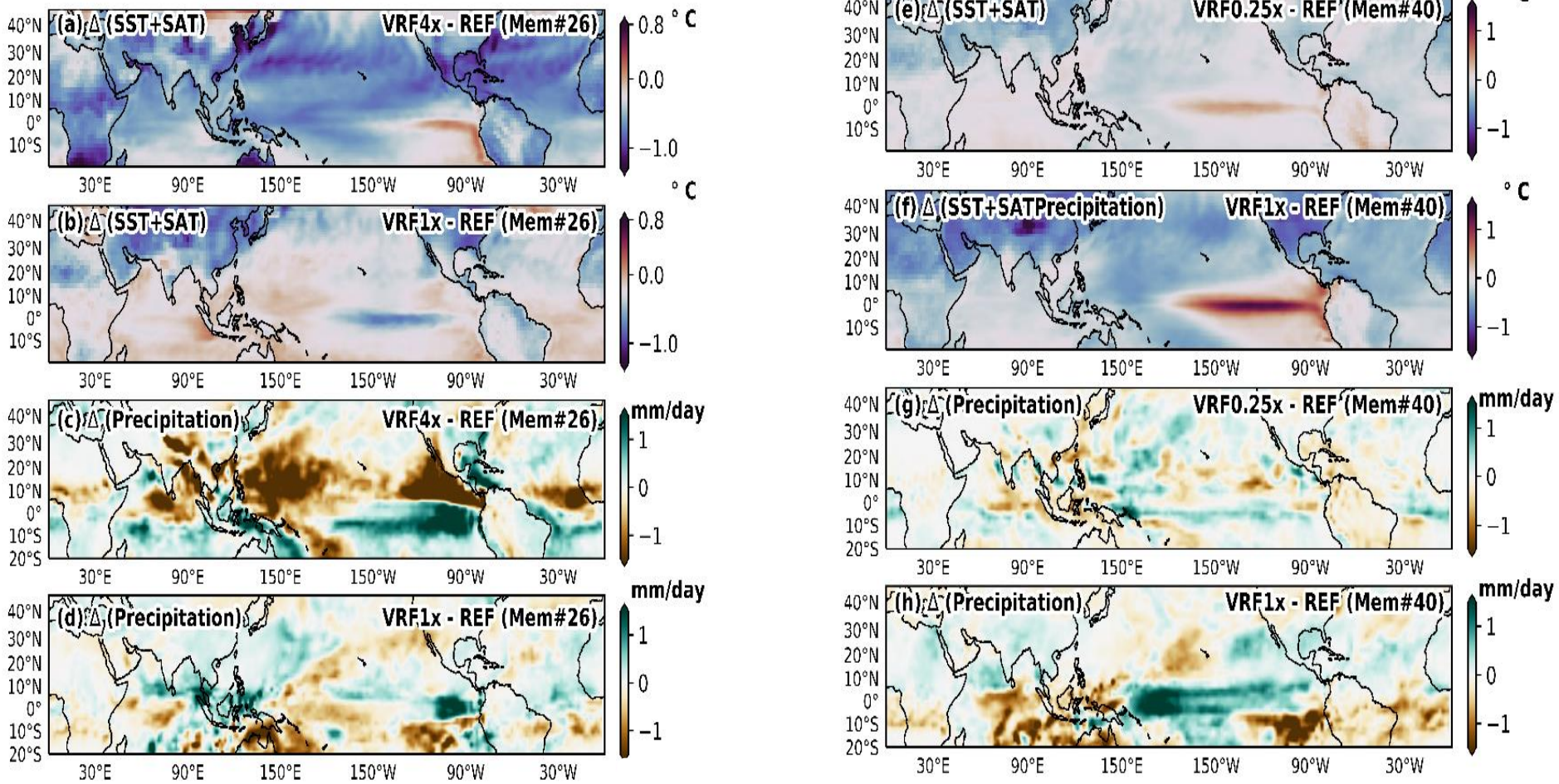

Bayesian Analysis

Paleoclimate proxies
of ENSO (14) and IM (11)

$$P(ENSO - IM\ co - occurrence|ENSO) = \frac{X+Y}{Z+W}$$

where,

X = Total count of drought events co-occurring with El Niño

Y = Total count of monsoon-excess events co-occurring with La Niña

Z = Total count of El Niños

W = Total count of La Niñas

Probability of ENSO - IM co-occurrence conditional to

- ENSO
- ENSO and LVE

$$P(ENSO - IM\ cooccurrence|\ (ENSO \cap Volcano\ (year = -n\ relative\ to\ co - occurrence)) = \frac{X+Y}{Z+W}$$

equation 5

X = Total count of drought events co-occurring with El Niño and eruption n years before El Niño-drought events

Y = Total count of monsoon-excess events co-occurring with La Niña and eruption n years before La Niña-monsoon excess events

Z = Total count of El Niños with eruption n years before El Niño

W = Total count of La Niñas with eruption n years before La Niña

- ENSO and PDO
- ENSO and PDO and LVE

Wilks, D.S., 2011. Statistical methods in the atmospheric sciences (Vol. 100). Academic press.

Bayesian analysis in the year following LVE

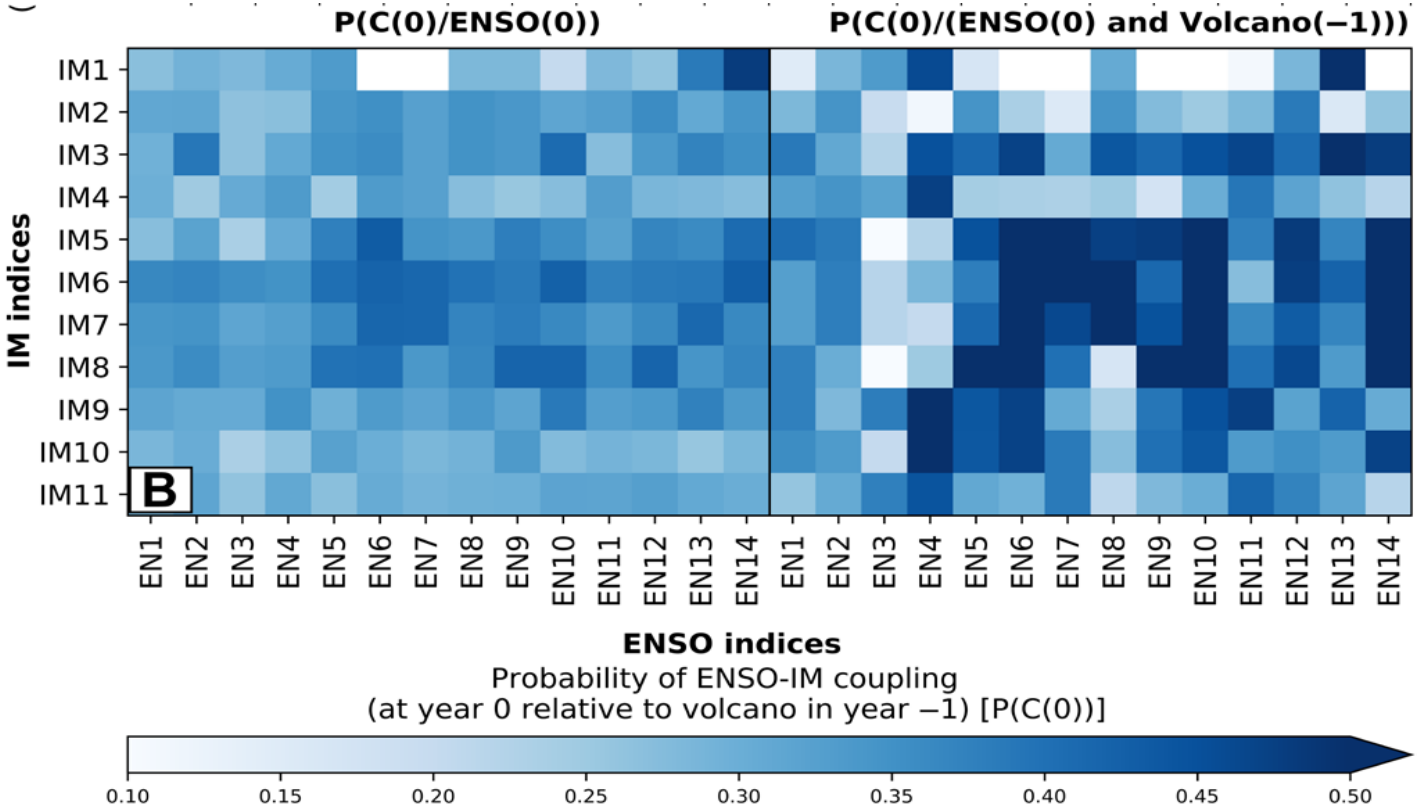

Probability of ENSO-IM coupling enhances in 93 (out of 149), more than doubling in a number of cases for last millenium

Manmeet Singh et al. 2020

MONSOON MISSION

A Targeted Activity to Improve
Monsoon Prediction across Scales

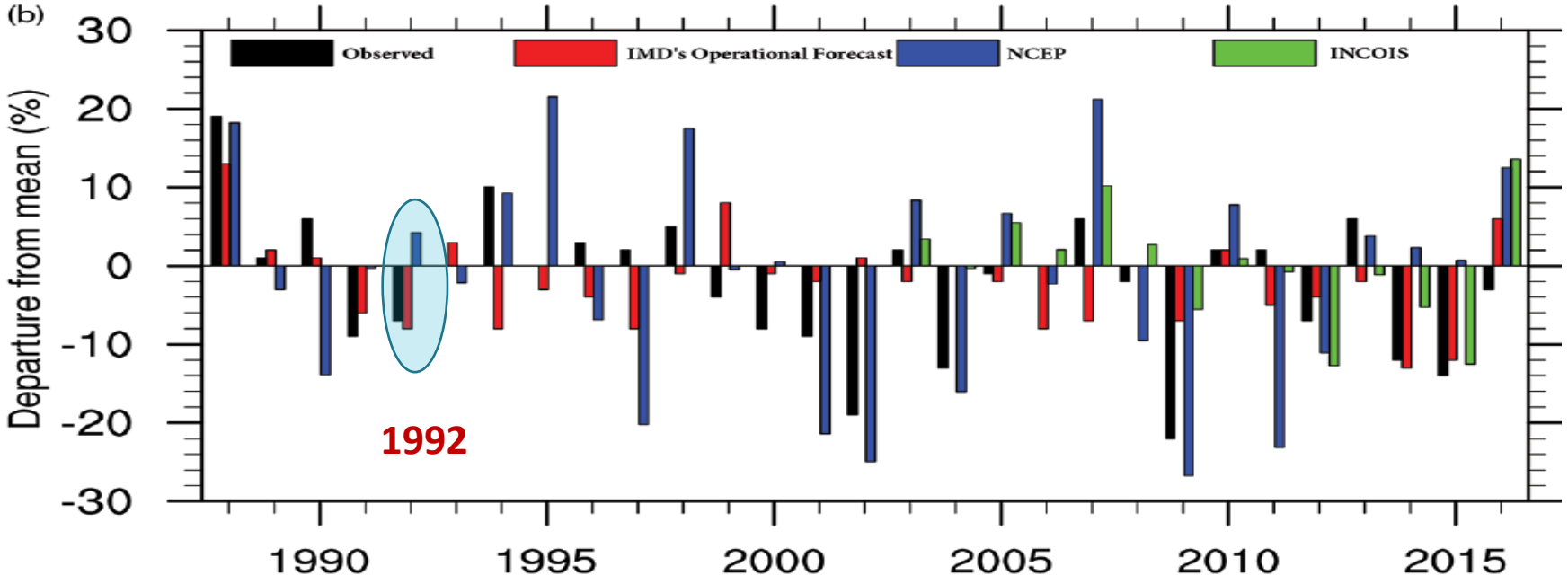

Comparison of observed ISMR, operational ISMR forecast based on IMD's statistical model , and MM CFSv2-T382-predicted (hindcast) based on NCEP & INCOIS initial conditions from 1988 to 2017. ISMR is calculated as the rainfall averaged over Indian land points only.

Rao et al., 2019, BAMS

Stratospheric aerosol optical depth at 550 nm

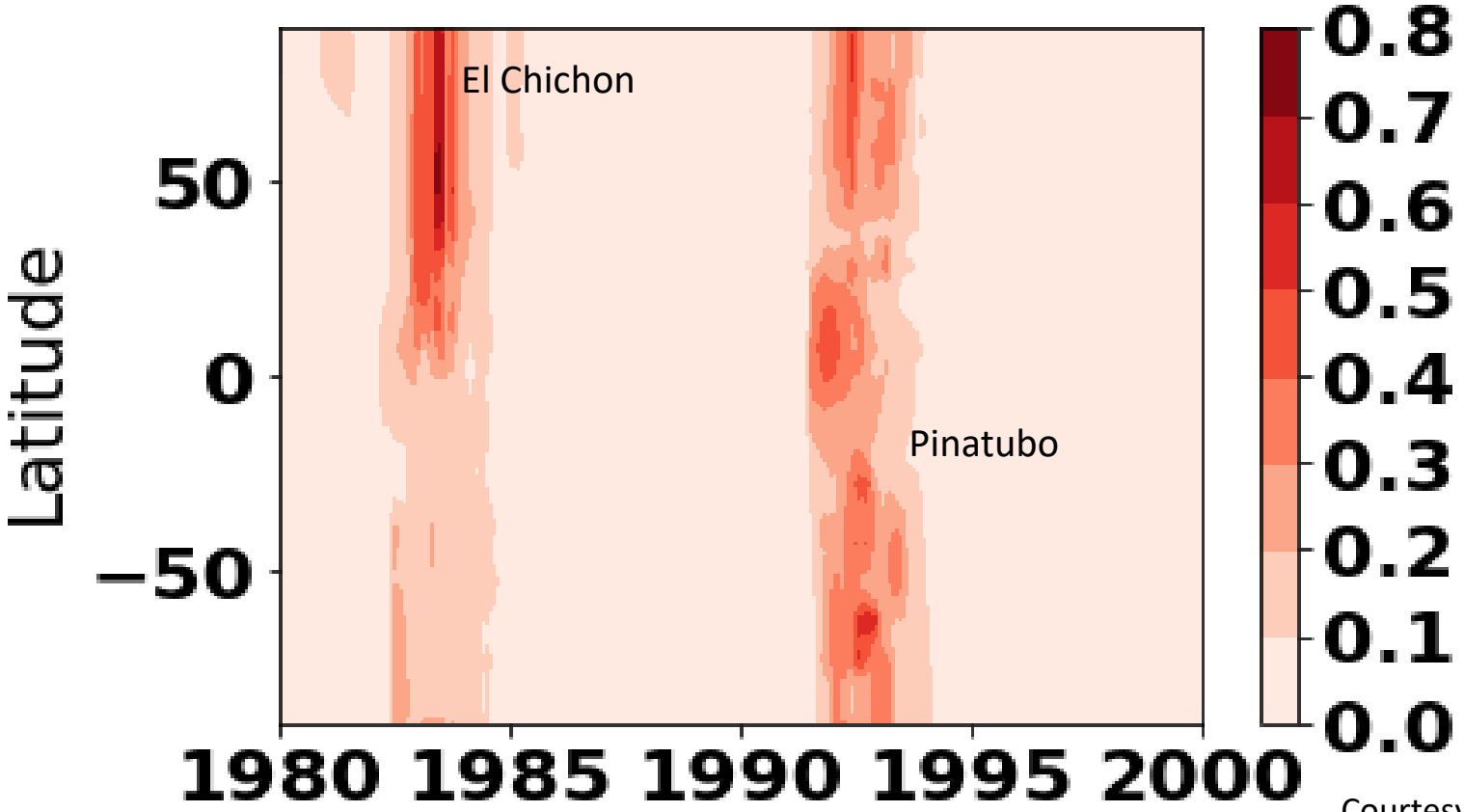

Courtesy: Manmeet Singh

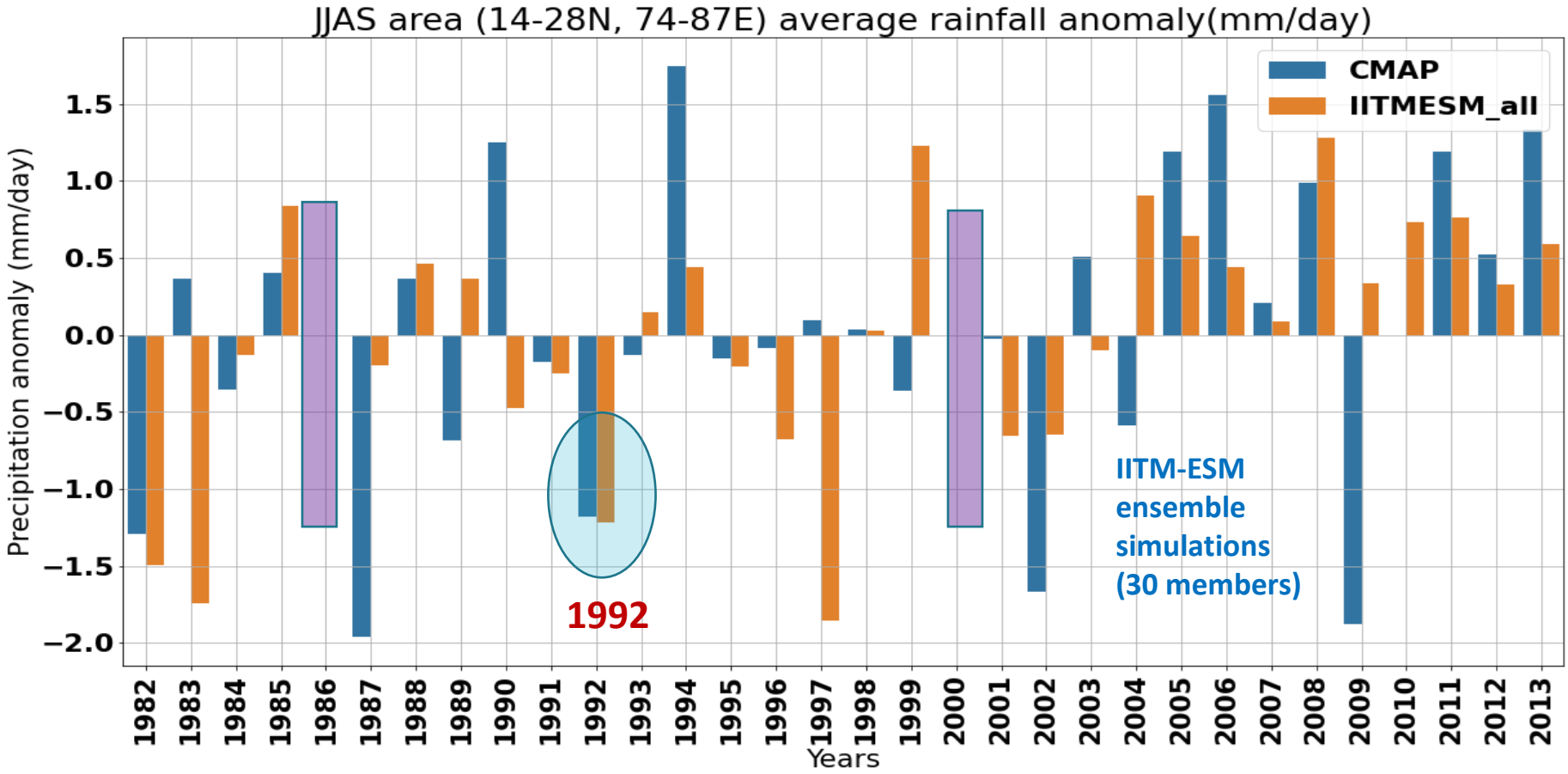

1986 and 2000 hindcasts to be done (TBD)

Courtesy: Manmeet Singh

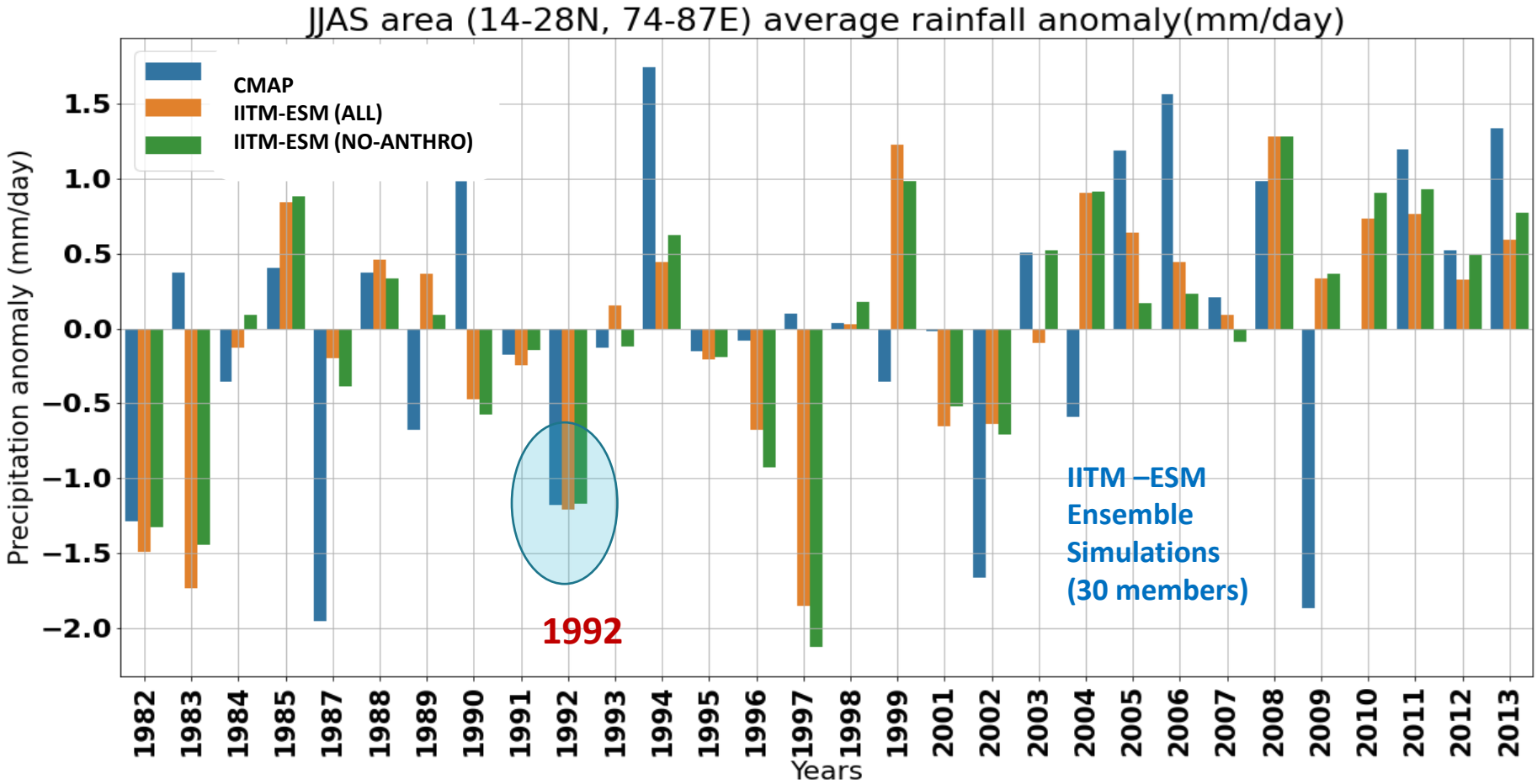

1986 and 2000 hindcasts to be done (TBD)

Courtesy: Manmeet Singh

JJAS 1992 precipitation anomaly

CMAP observations

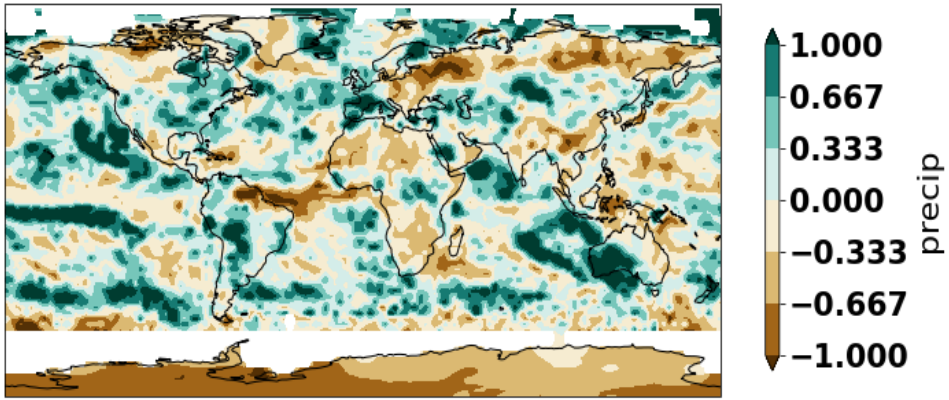

IITM-ESM anomaly

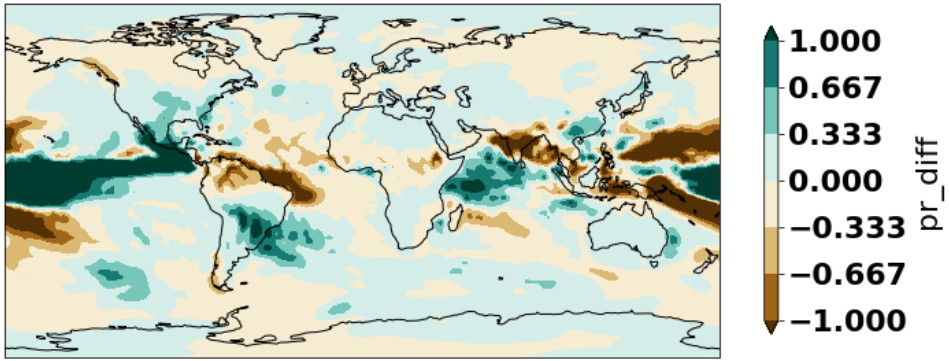

Courtesy: Manmeet Singh

Hunga Tonga – Honga Ha’apai eruption – January 2022

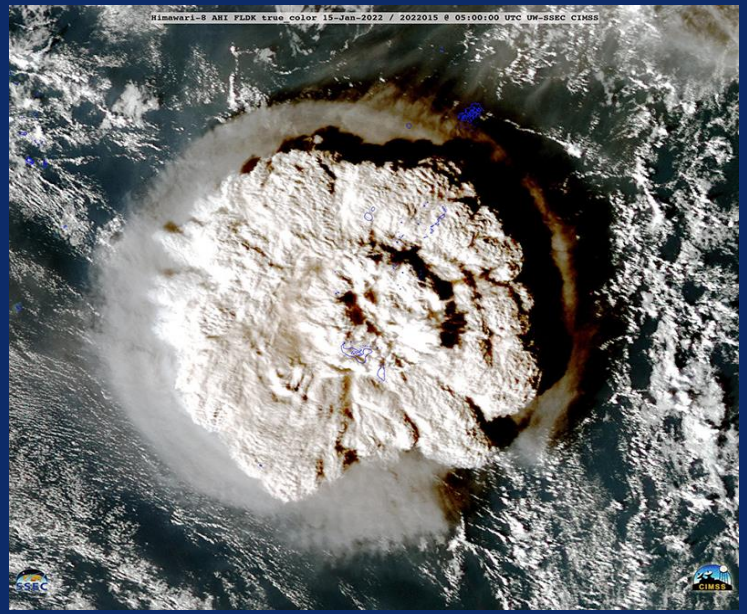

HIMAWARI-8 satellite image showing the significant eruption plume that rose from Hunga Tonga Hunga Ha’apai taken at 1800 (local time) on 15 January 2022. The top of the plume measured at least 600 km in diameter and rose to at least 20 km altitude, possibly higher. Tongan islands are outlined in blue. Courtesy of CIMSS.

In December 2021, an eruption began on Hunga Tonga–Hunga Haʻapai, a submarine volcano in the Tongan archipelago in the southern Pacific Ocean. The eruption reached a very large and powerful climax nearly four weeks later, on 15 January 2022.Hunga Tonga–Hunga Haʻapai is 65 kilometres (40 mi) north of Tongatapu, the country's main island (20.55°S, 175.385°W) . On the Volcanic Explosivity Index scale, the eruption was rated at least a VEI-5. Source: Wikipedia

The Hunga Tonga–Hunga Ha’apai eruption in 2022 propelled a record-breaking amount of water vapour into the Earth’s stratosphere.

Courtesy: National Institute of Water and Atmospheric Research (NIWA), New Zealand

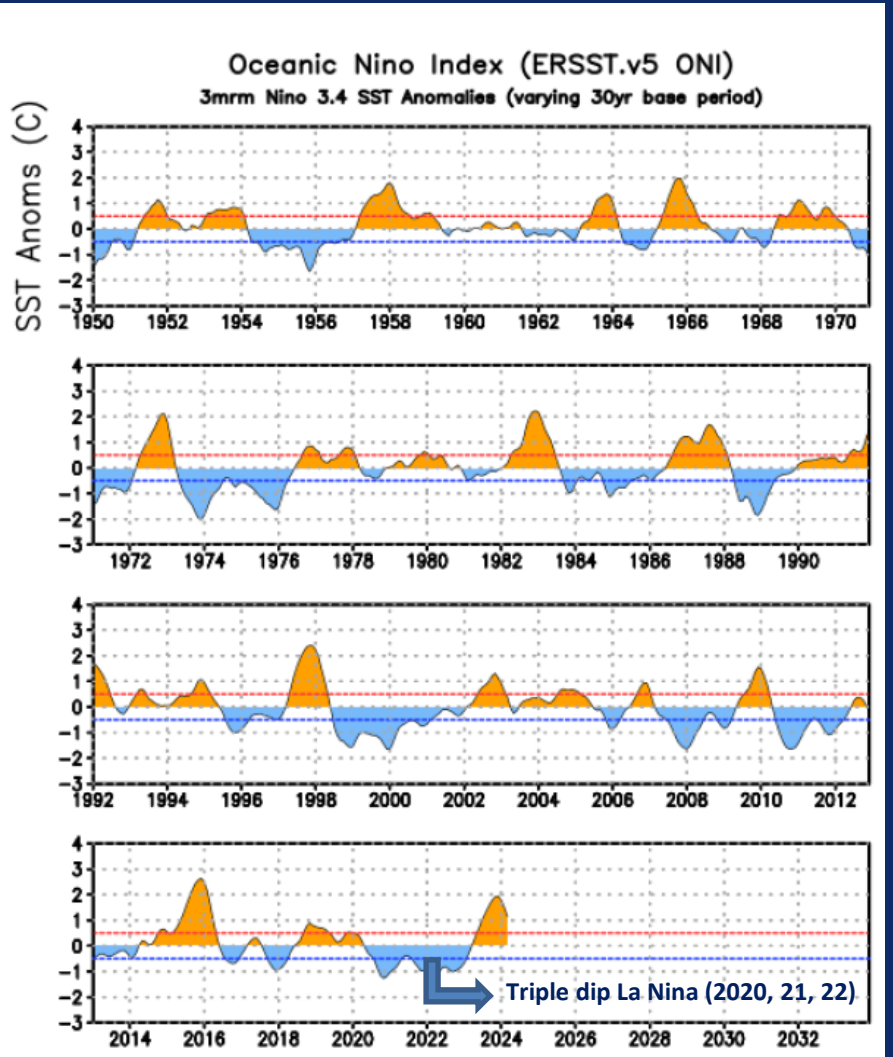

Oceanic Nino Index
ONI (°C): Evolution since 1950

Oceanic Niño Index (ONI) [3 month running mean of SST anomalies in the Niño 3.4 region (5°N-5°S, 120°-170°W)]

El Niño ↑

Neutral

La Niña ↓

The most recent ONI value (February – April 2024) is 1.1°C

Source: NOAA

Recent evolution of equatorial Pacific SST departures (°C)

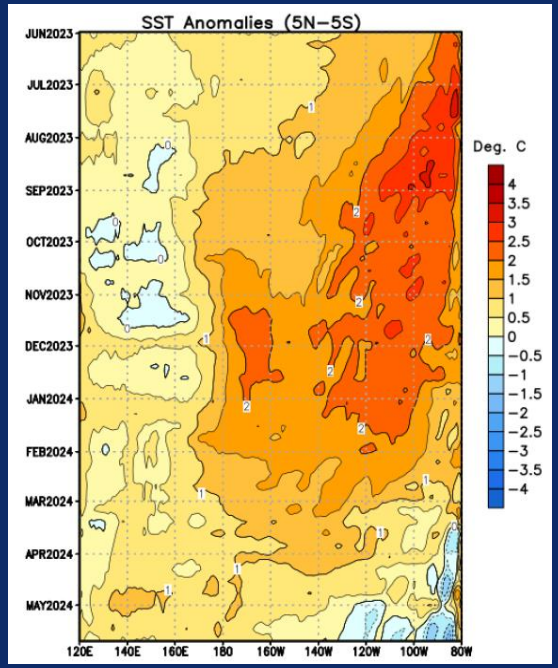

From March-October 2023, positive SST anomalies in the eastern Pacific Ocean gradually expanded & shifted westward.

In October and November 2023, SST anomalies increased in the central & east-central Pacific. Since late December 2023, positive SST anomalies have weakened across most of the Pacific.

Since mid March 2024, below-average SSTs have emerged in the eastern Pacific and have expanded slightly westward.

Nino region SST departures

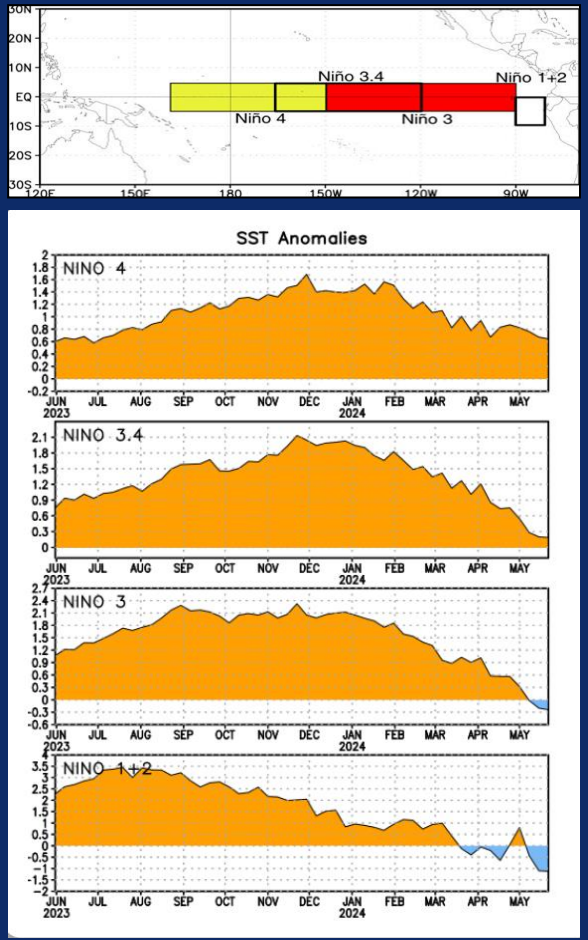

The latest weekly SST departures

SST departures (°C) in the Tropical Pacific during the four weeks (28 Apr 2024 - 25 May 2024)

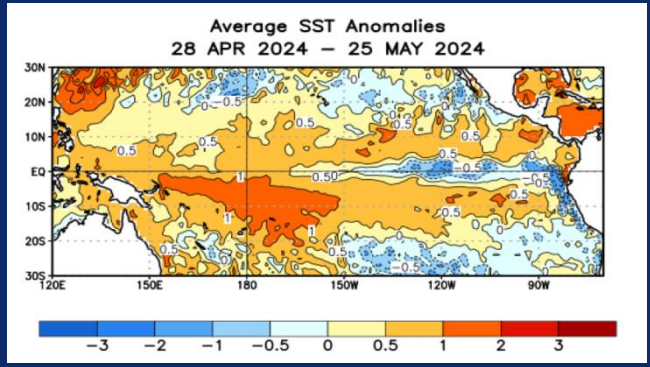

During the last four weeks, equatorial SSTs were above average across the western and central Pacific Ocean. Near-to-below average SSTs were evident in the east-central and eastern Pacific Ocean

Source: NOAA

Recent evolution of equatorial Pacific SST departures (°C)

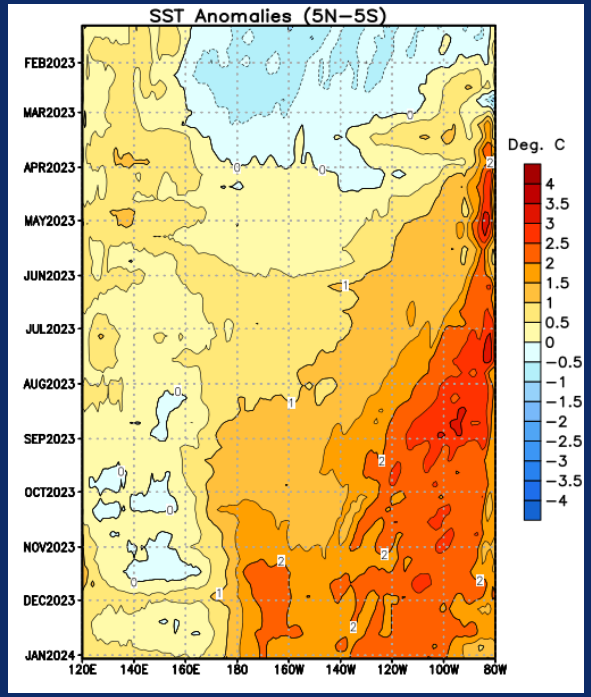

Since March 2023, positive SST anomalies in the eastern Pacific Ocean gradually expanded and shifted westward.

In October & November 2023, SST anomalies increased in the central and east-central Pacific. Since early December, the positive SST anomalies have persisted.

In the far eastern Pacific, positive SST anomalies have been gradually weakening.

Nino region SST departures

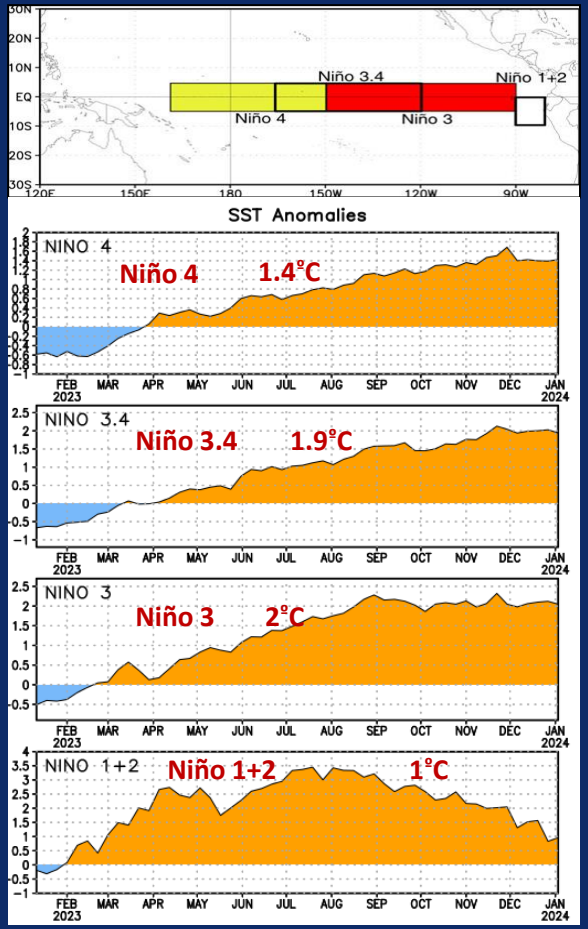

The latest weekly SST departures

SST departures (°C) in the Tropical Pacific during the four weeks (10 Dec 2023 - 6 Jan 2024)

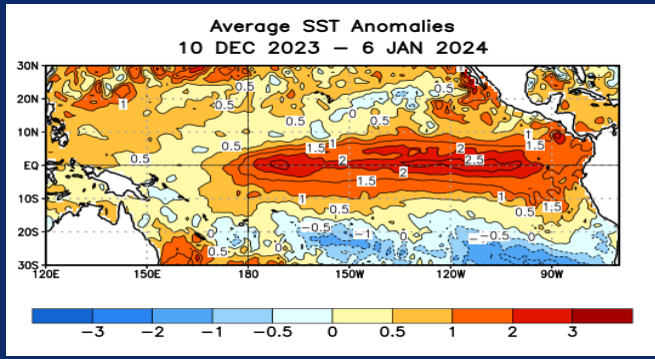

In the last four weeks, equatorial SSTs were above average across most of the Pacific Ocean, with near-average SSTs in the western Pacific Ocean

Source: NOAA

IRI Pacific Niño 3.4 SST Model Outlook

The majority of models indicate ENSO-neutral will persist through July-September 2024. Thereafter, most models indicate a transition to La Niña around August-October 2024.

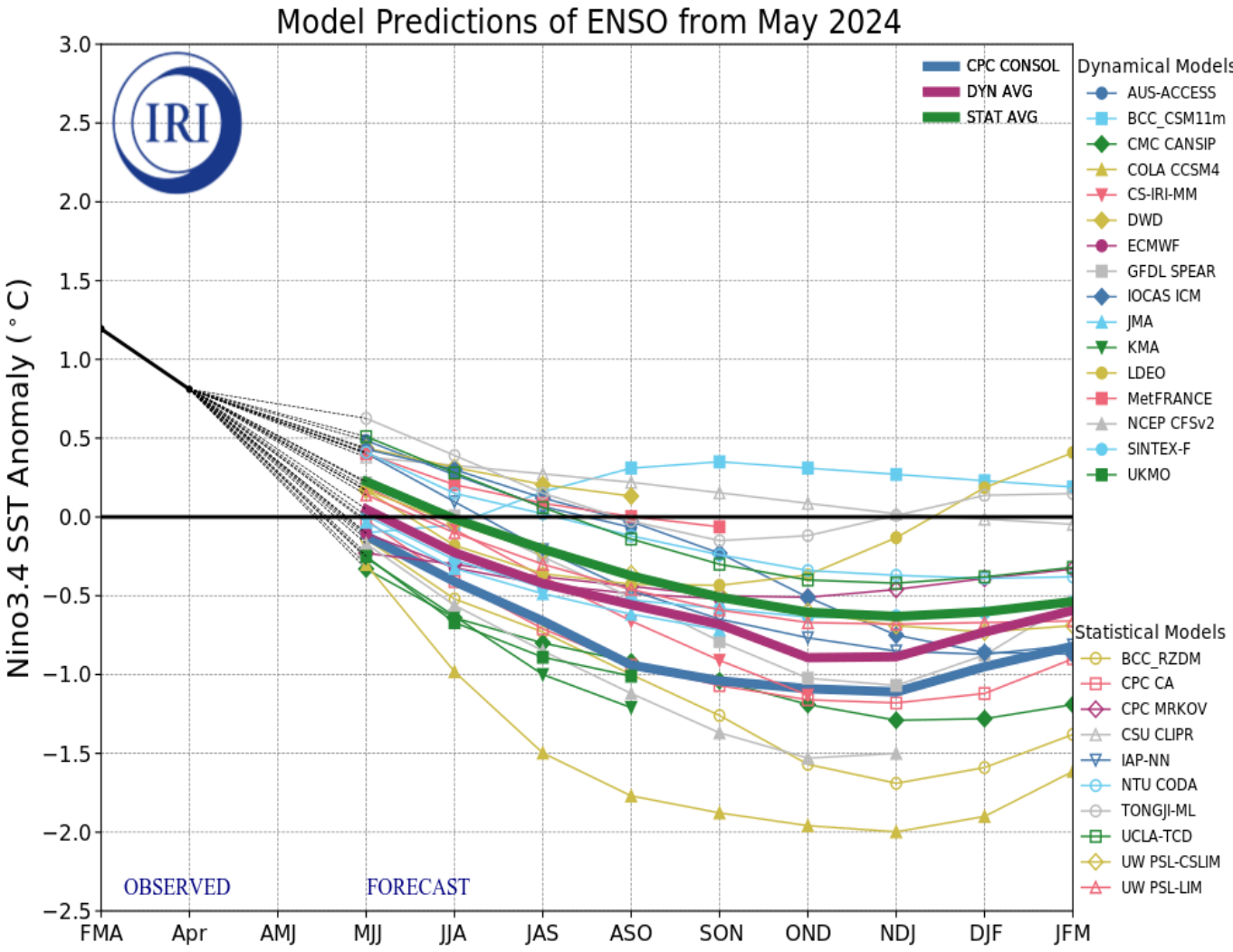

2023 Seasonal (June – September) Rainfall and its Anomaly

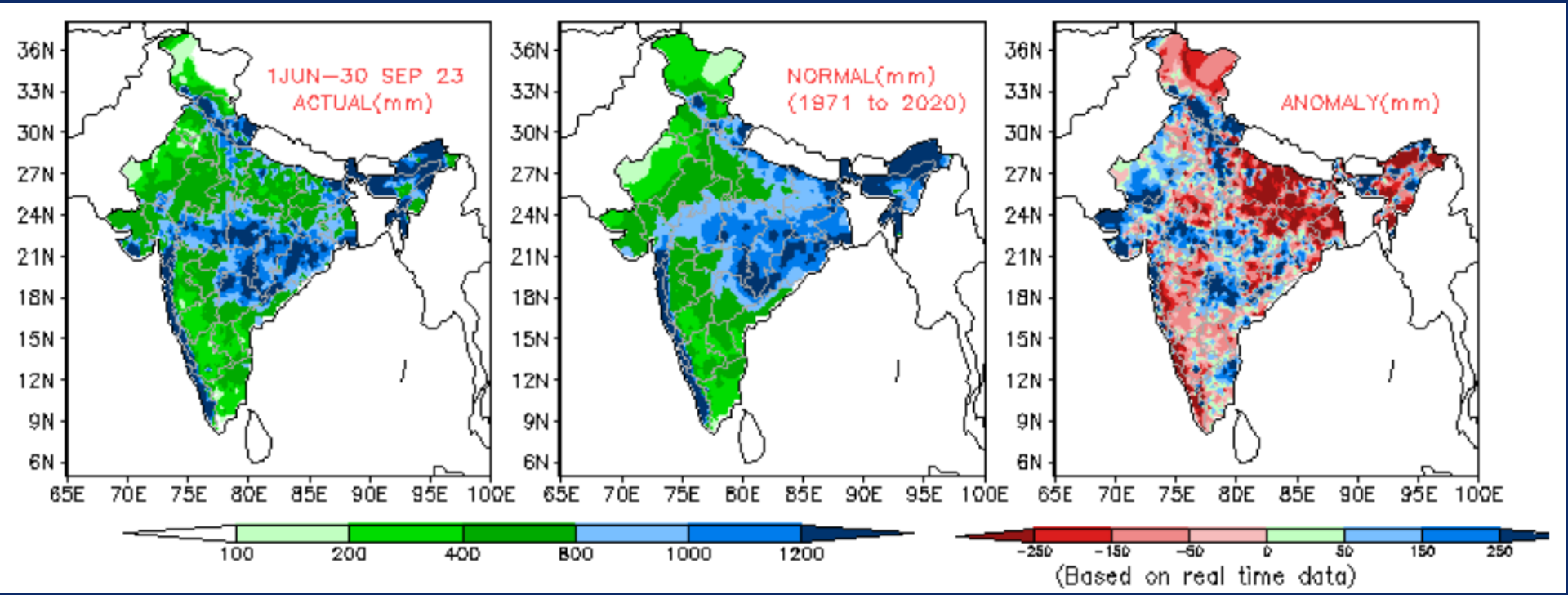

Source: India Met Dept (IMD)

Hunga Tonga – Honga Ha'apai eruption : Role on the 2023 El Nino and Indian monsoon ?

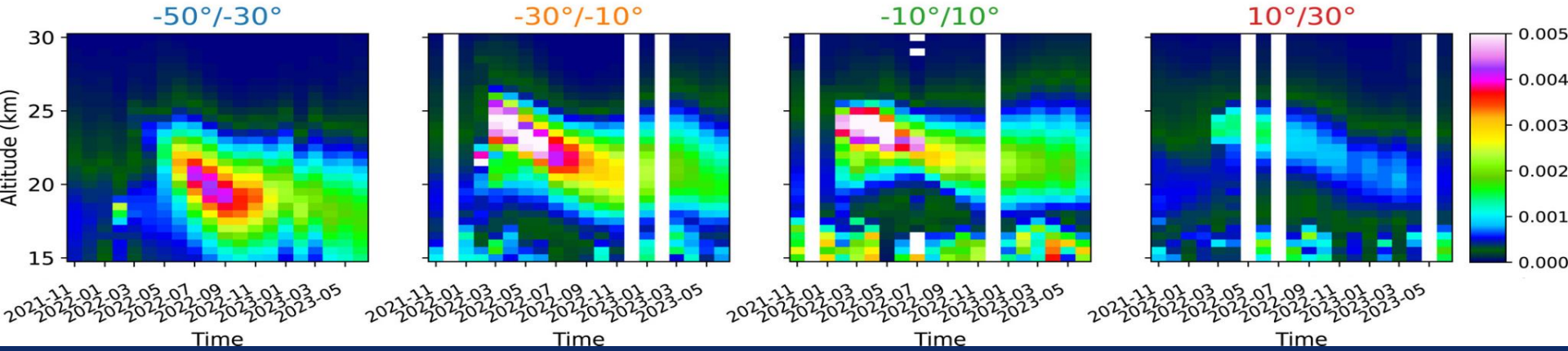

Zonal altitude-time sections of aerosol extinction *kext* (km^{-1}) provided by SAGE III at 755 nm. The cross-sections are averaged over 20° latitude bands between 50°S and 30°N from November 2021 to June 2023.

Ref: Duchamp, C., Wrana, F., Legras, B., Sellitto, P., Belhadji, R., & von Savigny, C. (2023). Observation of the aerosol plume from the 2022 Hunga Tonga—Hunga Ha'apai eruption with SAGE III/ISS. Geophysical Research Letters, 50, e2023GL105076

Transition from La Nina to ENSO-Neutral in Feb 2023

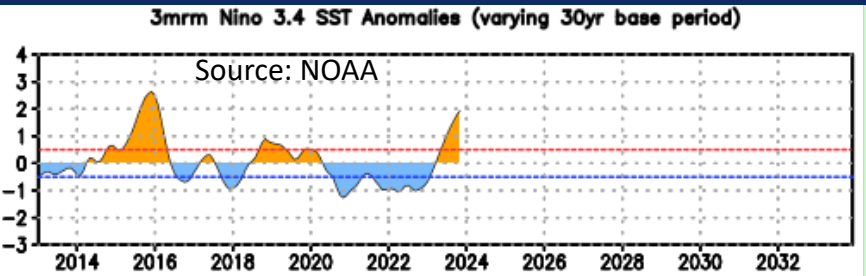

Time series of the 2023 All India Summer Monsoon Rainfall

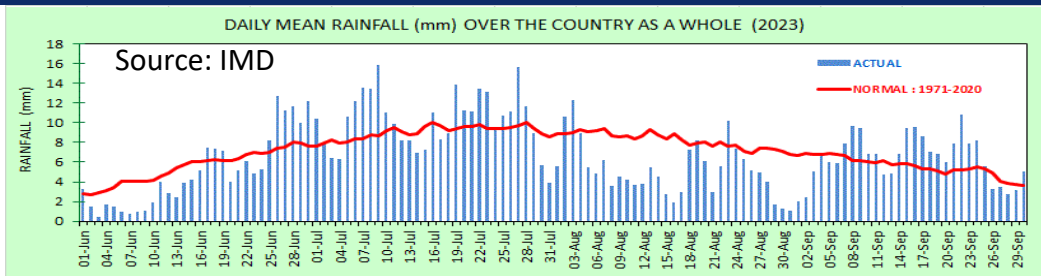

Summary

•Indian Monsoon (IM) can be better predicted after large volcanic eruptions (LVE) – S2S time-scales

- As erratic as they are, volcanic eruptions improve the predictability of IM, due to a stronger coupling between the monsoon over large parts of South and South-East Asia and the El Niño phenomenon after an eruption. The present findings now suggest a novel, additional path for monsoon predictions that are crucial for agricultural planning in India.
- Combining data from meteorological observations, climate records, computer model simulations, and paleoclimate archives such as tree-rings, corals, cave deposits and ice-cores from past millennia of Earth history, it is found that a synchronization of the monsoon with the strongest mode of natural climate variability, the El Niño, makes it easier to anticipate the strength of seasonal rainfall in the Indian subcontinent.
- The tiny particles and gases that a large volcano blasts into the air enter into the stratosphere and remain there for a few years. While the volcanic matter in the stratosphere to some extent blocks sunshine from reaching the Earth's surface, the reduced solar forcing increases the probability of an El Niño event in the next year. This is because less sunshine means less warmth and hence a change of temperature differences between the Northern and Southern hemisphere, which in turn affects the atmospheric large-scale circulation and precipitation dynamics.
- Advanced data analysis now reveals that LVEs are more likely to promote the coincidence of warm El Niño events over the Pacific and Indian monsoon droughts – or, in contrast, cool La Niña events over the Pacific and Indian monsoon excess.
- The synchronization between ENSO and IM is changing over time, with human-made global warming being one of the factors, worsening the accurate predictions of the monsoon.

•Regional implications of geo-engineering experiments

- To reduce global warming from human-made greenhouse gases, some scientists envision solar radiation management (SRM) – basically to block a portion of sunrays from warming Earth's surface by putting aerosols / light scattering materials in the stratosphere, similar to what the natural phenomenon of a volcanic eruption does.
- Artificially blocking sunshine, however, might dangerously interfere with a number of processes in the atmosphere, such as the Indian Monsoon. Understanding the mechanisms at play is thus important. It also raises a number of important scientific questions that need to be addressed.

Thank you for your kind attention !